KASDI MERBAH UNIVERSITY – OUARGLA
Faculty of Hydrocarbons, Renewable Energies, Earth Sciences, and Universe
Department of Exploration and Petroleum Workshop Mechanics

Professional Master's Thesis

Domain: Hydrocarbons

Petroleum Workshop Mechanics

Presented by:

- **Bouzidi Younes**
- **Aouiche Houssem**
- **Triek Riyad**

Super visor: Belloufi youcef

Improvement of braking system performance in drilling rig operations

Publicly defended on:

14-06-2023

Before the jury:

Ex: Helal Yazid

Pr: Frouhat

Academic year: 2022-2023

Acknowledgment:

We humbly express our gratitude to Allah for His boundless guidance and assistance that have enabled us to reach this stage in our academic journey.

Our supervisor, Dr. Belloufi Youcef, has played an instrumental role in the success of this project. His unwavering support and invaluable guidance have been the cornerstone of our progress. We are deeply indebted to him for his patience, expertise, and encouragement, which have propelled us through every phase of this research.

We also extend our sincere appreciation to the esteemed members of the jury for their diligent review of our dissertation. We recognize their valuable time and effort invested in evaluating our work, and we are grateful for the opportunity to present our defense before such a distinguished panel. Their constructive feedback and insightful suggestions have enriched our research and deepened our understanding of the subject matter.

We consider ourselves fortunate to have had the honor of working under the guidance of Dr. Belloufi Youcef and being evaluated by such a knowledgeable and experienced jury. We will carry the lessons we have learned throughout this process with us throughout our academic and professional careers.

Table of Contents:

CHAPTER III

CHAPTER IV

List of Figures:

CHAPTER I

CHAPTER II

CHAPTER III

CHAPTER IV

List of tables

CHAPTER I

CHAPTER II

CHAPTER IV

Abstract:

This message presents a study that explores the utilization of a heat exchanger (water/soil) to cool the brake system in a driveworks system. The primary aim is to ensure a consistent distribution of heat within the soil along the water channel by applying the heat conduction equation and energy balance. An analytical model was proposed to determine water temperatures across the exchanger under a constant heat transfer condition, while a numerical model utilizing the finite difference method was developed for convective heat transfer. To validate the accuracy of both analytical and numerical models, an experimental study was conducted at the University of Ouargla, yielding qualitative and quantitative agreement during the verification process. Positive outcomes were observed in terms of improving the brake system's efficiency.

Keywords: Water-Soil Heat Exchanger, Brake Cooling, Analytical Equations, Increased System Efficiency.

ملخص :

تتناول هذه الرسالة دراسة استخدام المحول الحراري من نوع (ماء/تربة) في عملية تبريد فرامل نظام الدراووركس. الهدف الرئيسي هو تحقيق توزيع متساوٍ للحرارة داخل التربة على امتداد القناة المائية باستخدام معادلة الحرارة والحوصلة الطاقوية. تم اقتراح نموذج تحليلي لتحديد درجات حرارة المياه عبر المحول في حالة نقل الحرارة الثابتة، وتم تطوير نموذج عددي للنقل الحراري الانتقالي باستخدام طريقة الفروق المنتهية الضمنية. تم إجراء دراسة تجريبية في جامعة ورقلة للتحقق من صحة النماذج التحليلية والعددية المستخدمة، وتم تحقيق توافق نوعي وكمي خلال عملية التحقق. تم تحقيق نتائج إيجابية في زيادة كفاءة نظام المكابح .

الكلمات المفتاحية: المحول الحراري ماء-ارض، تبريد الفرامل، الدراووركس، المعادلات التحليلية، زيادة كفاءة النظام.

Nomenclature

symbols	designation	Unite
T_{soil}	soil temperature	$°C$
T_i	initial Temperature the interior of the soil	$°C$
s	Exchange surface	m^2
λ_{soil}	Thermal conductivity of the soil	W/m.K
h	Average convective heat transfer coefficient of the water	W/m^2. K
δ	Heat penetration depth into the soil	m
m	Mass of water	kg
ṁ	Mass flow rate of water	kg/s
cp	Specific heat capacity	j/kg.K
u	Axial velocity of air inside the heat exchanger	m/s
r_1	Inner radius of buried tube	m
r_2	Outer radius of buried tube	m
r_3	Radius of the adiabatic layer of the soil	m
l	Radius of the adiabatic layer of the soil	m
x	Horizontal coordinate	m
α	Thermal diffusivity	m^2/s
z	Vertical coordinate	m
ρ	Density	Kg/m^3
R	Thermal resistance	m.K/W
ε	effective efficiency	

General introduction:

Drawworks are essential components of oil and gas drilling rigs, responsible for efficiently raising and lowering heavy equipment and the drill string. They provide the necessary power and control, ensuring safe rig operation and productivity, Water-earth heat exchangers offer sustainable and efficient cooling solutions by utilizing the ground's constant temperature to cool water used in their cooling system. By circulating water through underground pipes, heat is absorbed from the soil, allowing for effective cooling without relying solely on conventional methods. With their environmentally friendly operation and energy-saving potential, water-earth heat exchangers are gaining popularity in residential, commercial, and industrial applications as a greener cooling alternative.

As part of our research and its summary in the form of a graduation thesis, we have divided it into four chapters, all focused on the topic of developing the braking system in drawworks.

Chapter 1 of our research focuses on the foundational concept that gave rise to the drawworks and its significance within the oil and gas industry. We examine the key components that comprise the drawworks system and explore their roles and functions. Additionally, we delve into the crucial role of heat exchanges, with a specific emphasis on the water-earth heat exchanger and its importance in the context of drawworks.

In chapter 2 we provided a comprehensive overview of the existing literature on this sustainable and efficient cooling technology. This analysis examines various research articles, academic papers, and technical reports that explore the design, performance, and applications of water-earth heat exchangers. By reviewing the available literature, this analysis aims to identify trends, advancements, and challenges in the field, offering valuable insights for further research and development. The analysis also highlights the environmental benefits, energy savings potential, and practical considerations associated with the implementation of water-earth heat exchangers in different settings.

Chapter 3 focuses on the mathematical modeling and numerical simulation of water-earth heat exchangers. This chapter explores the process of developing mathematical equations that accurately represent the heat transfer dynamics within these systems. By implementing numerical methods and simulation techniques, researchers can analyze and optimize the performance of water-earth heat exchangers under different operating conditions. This chapter provides valuable insights into the behavior of these heat exchangers and offers a platform for studying their efficiency, thermal performance, and potential for sustainable cooling applications.

Chapter 4 provides an experimental view of the subject matter. This chapter focuses on conducting practical experiments to validate and complement the theoretical aspects discussed in previous chapters. By implementing various experimental setups and methodologies, researchers can obtain real-world data to verify the performance and effectiveness of water-earth heat exchangers. The chapter highlights the importance of experimental investigations in gaining a comprehensive understanding of the system behavior and provides valuable insights for practical applications.

Chapter I

Generality

History:

The drawworks has come a long way since its humble beginnings as a simple windlass or winch. Today, it is a highly sophisticated piece of equipment that is responsible for the vital task of hoisting drill stem and casing out of the depths of the earth during oil and gas drilling operations. The drawworks is a critical component of drilling rigs and is rated based on its horsepower by the oil and gas industry.

Over time, the drawworks has evolved from relying on steam engines to power the hoist, to modern rigs utilizing diesel engines and electric motors. Despite these advancements, the basic principle of using a mechanical device to lift heavy loads remains the foundation of hoisting[1].

The drawworks is highly valued in the oil and gas industry for its compact structure, straightforward transmission, large transferred power, effective performance, convenient installation and adjustment, easy maintenance, and safe and reliable operation. Its numerous critical operations make it an essential component at the very heart of drilling operations[2].

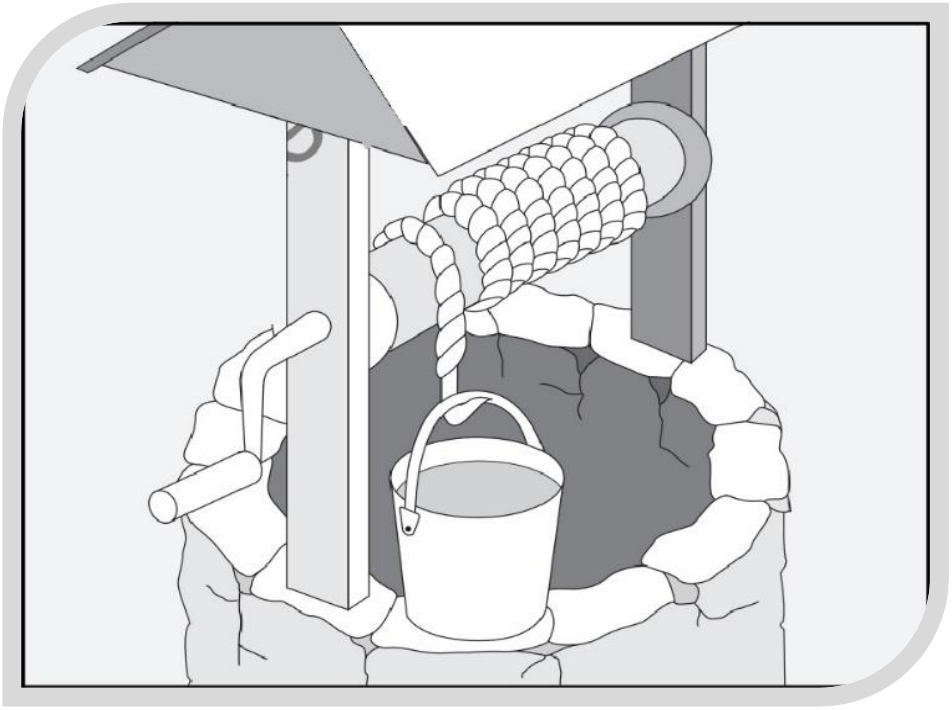

Figure 2 Windlass[1]

This chapter aims to illuminate the inner workings of the drawworks, beginning with the operating principles and components that define its role in the drilling rig ecosystem.

I. Components of a drawworks:

Numerous configurations of power sources, transmission, brakes, hoisting drum and block assembly allow the rig designer to outfit a draw-works to closely match the projected drilling conditions[1] .

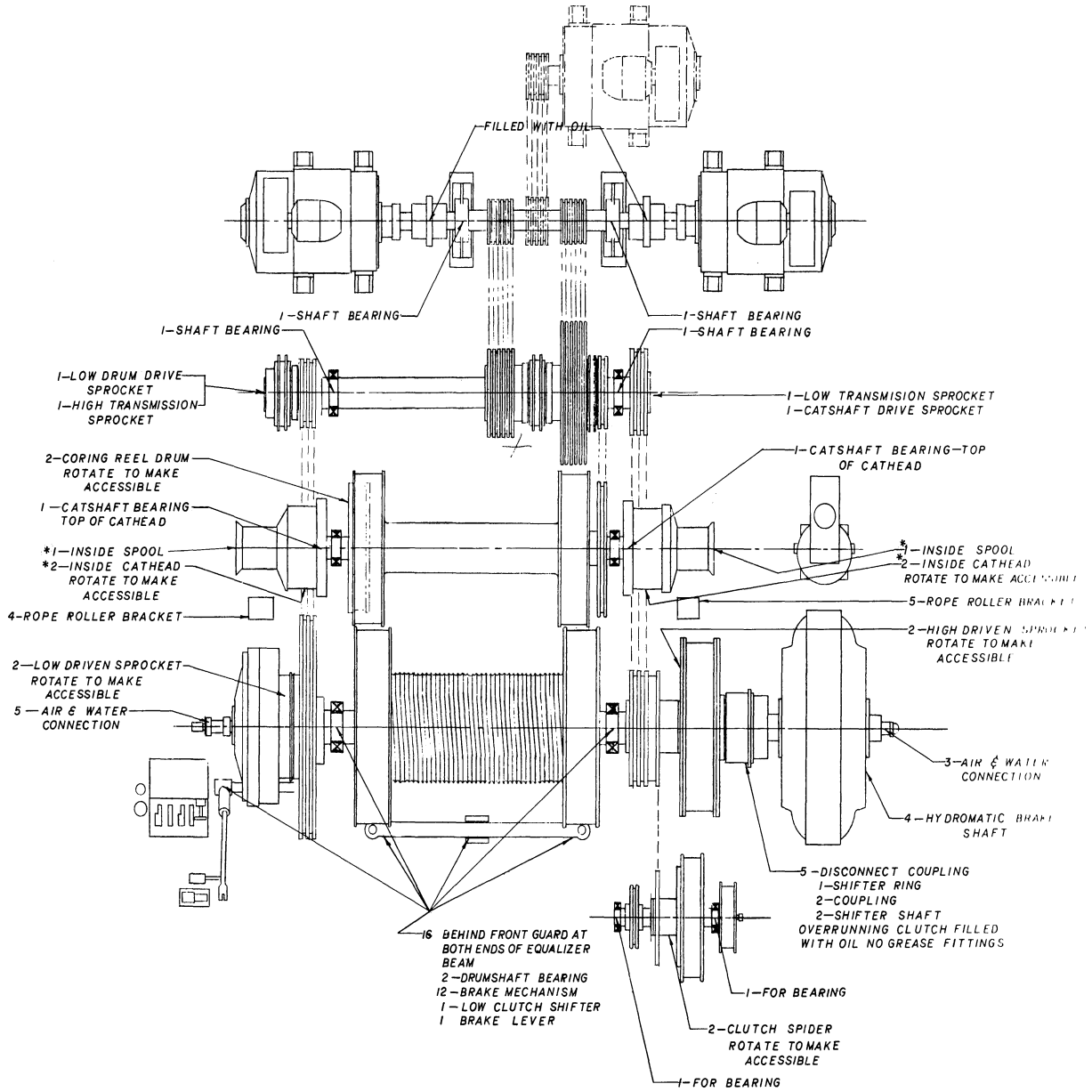

Figure 2 *: schematic drawworks [2]*

II. Details on the main set components of the drawwork:

II.1. Power source: Depending on the engines on the rig, the drawworks can be either:

II.1.1. MECHANICAL:

Diesel engines are directly connected (compounded) to the drawworks by chain. This system is still in use for small Drilling Rigs (under 1500 HP), but is no longer used on medium-Hi powered rigs(1500 & 3000 HP) [3] .

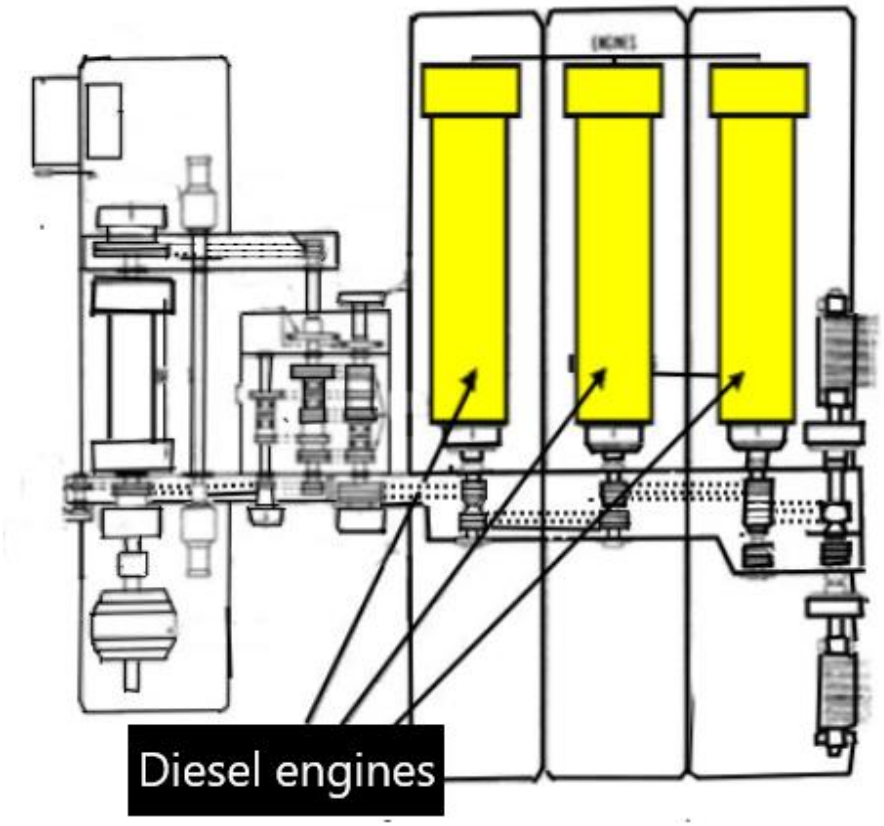

Figure3 schematic of diesel power source

II.1.2. ELECTRICAL:

Electrical systems are normally used today on land rigs and is the only system in use on offshore rigs. The drawworks are generally connected to 1000 HP D.C. engines, although A.C. engines are now being used as well[3] .

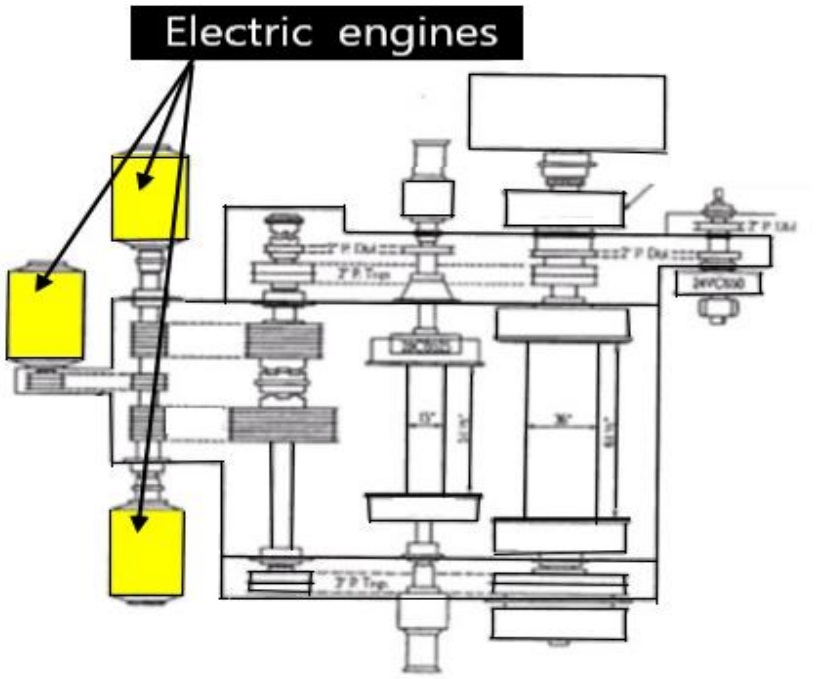

Figure 4: schematic of electrical power source

II.2. Drawworks body :

Drawworks frame is wall plate welded substructure which can position acutely and support motor, drum shaft, gear reducer, automatic driller and hydraulic disk. drawworks frame consists of frame and skid. It's welded by structural section and inner wall plate is welded to the skeleton by channel steel, and it is welded by structural sections.

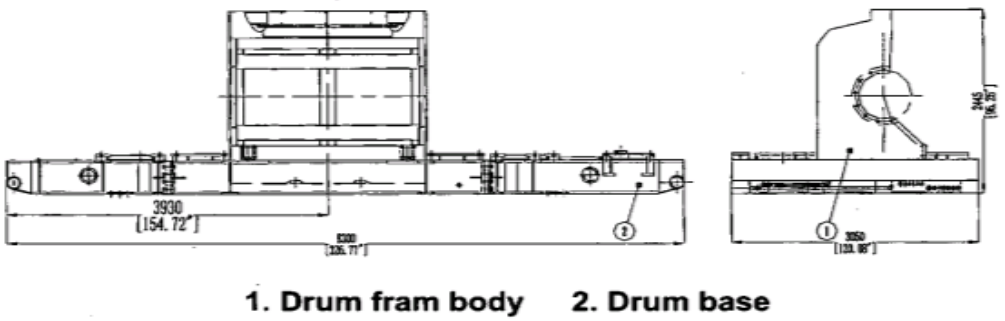

Figure 5 : Drawworks frame[4]

Drawworks' main base beam is made of a steel, welded framework. Set lifting lugs around the drawworks, cover the bottom of the drum body with a steel plate to prevent oil pollution from leaking out, and place the oil tank for the left and right gear reducers behind the right side of the case. All of the air, oil, and water pipelines are also organized inside the base, and the base has detachable covers installed in certain inspection-required locations [4] .

II.3. Main drum:

The drum ensures the easiest rolling of the drilling line to prevent it from disgorging while drilling, the main drum is perfectly balanced to minimize the vibrations caused by the fast acceleration.

The diameter of the main drum is a function of the diameter of the drilling line being used. It is preferable to have the drum as large as possible to reduce the number of wraps and the bending of the cable[5] .

The length of the drum is a function of the distance _ between Crown block and Drawworks. To reduce the wear on the drilling line, it is good practice to keep the angle alpha under degrees.

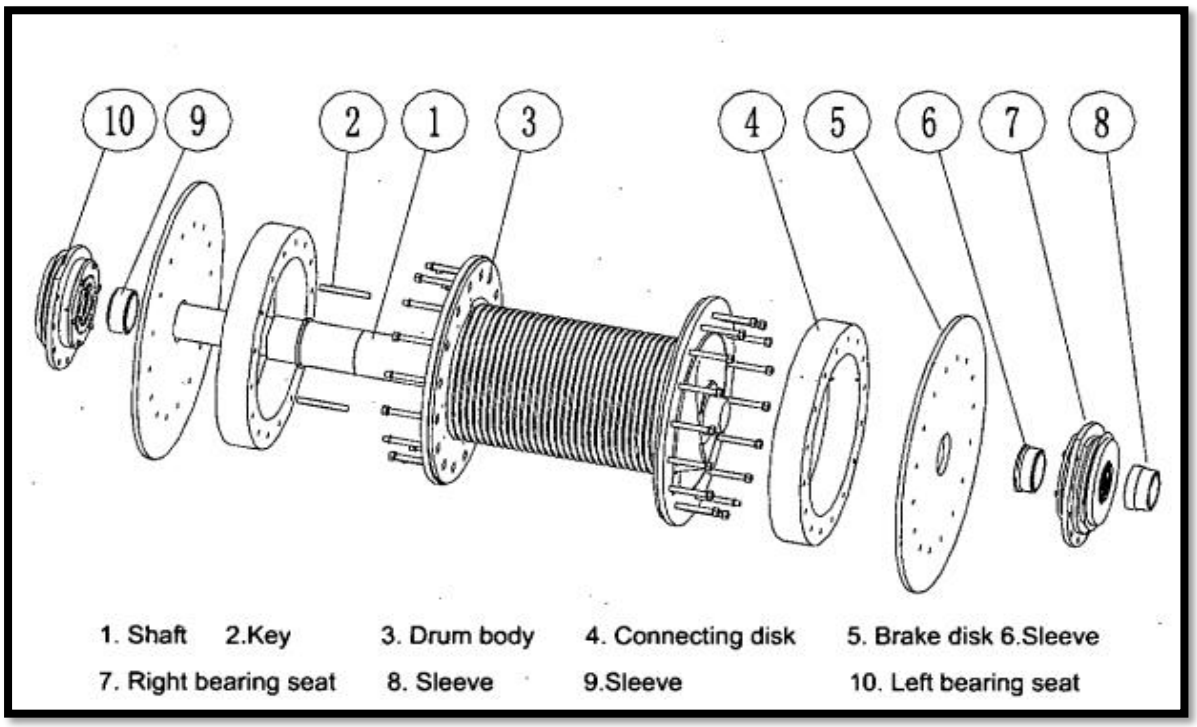

Figure 6: schematic of a drum

II.4. Transmission System:

It is the present practice to provide a speed transmission between the engine or source of power of a drilling rig and the various pieces of equipment The transmission usually embodies an input shaft, which is driven by the engine or source of power, and an output shaft, which is intended to be operated at various speed ratios The drawworks of the drilling rig is usually provided with two connections to the output shaft of the transmission

A further object of the present invention is to provide a transmission which PROVIDE MULTIPLE speed ratios usually available for driving various equipment of a drilling rig, such as a rotary table, front drum, etc [6] .

II.4.1. The shafts:

II.4.1.1. Input shaft: it's the one that receives the power from the power source then transmits it to the output shaft, dual chain of three rows is related to the engine allows it to turn at a speed of 602 RPM, an inert brake is placed nearby which allows rotation stop while changing the gears.

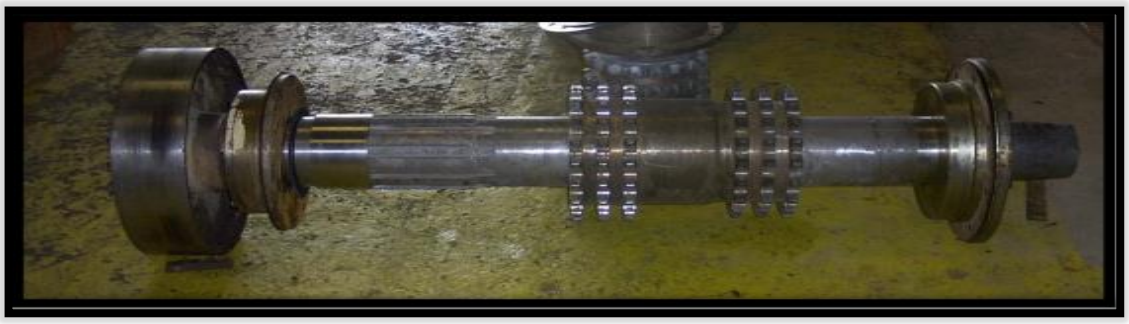

Figure 7: Input shaft[5]

II.4.1.2. Output shaft: it's related to the input shaft with two chains each one with three rows, this configuration allows us to get two speed rations: High 457 rpm and Low 285 rpm

The input and the output shafts are the components of the drawworks Gearbox

II.4.1.3. Drum shaft : drum shaft assembly is the key component of drawworks , it allows the the traveling system wireline onto the drum to be winded or withdrawn onto or from the drum by the clockwise or counter clockwise , its connected to the gearbox with two chains of 3 rows on opposite sides of the shaft (on the right side : high speed , left side : low speed) generating 4 speed rations (TABLE 1) [5].

SPEED (rpm)		DRUM CLUTCH	
		Low	High
input shaft spline	Low	65	243
	High	105	393

II.4.1.4. Cathead shaft: its related to the drum shaft with one chain of one row , generating two speed rations : LOW 102 rpm ; HIGH 195 rpm .

II.4.2. Chains:

the chains used in the drawworks are classified in 'OIL FIELD' category because of all the centrifugal force applied to it , this allows to get multiple speed rations to transmit which is considered as an important key in the drawworks mechanism as shown in the table 2 at the bottom [5] .

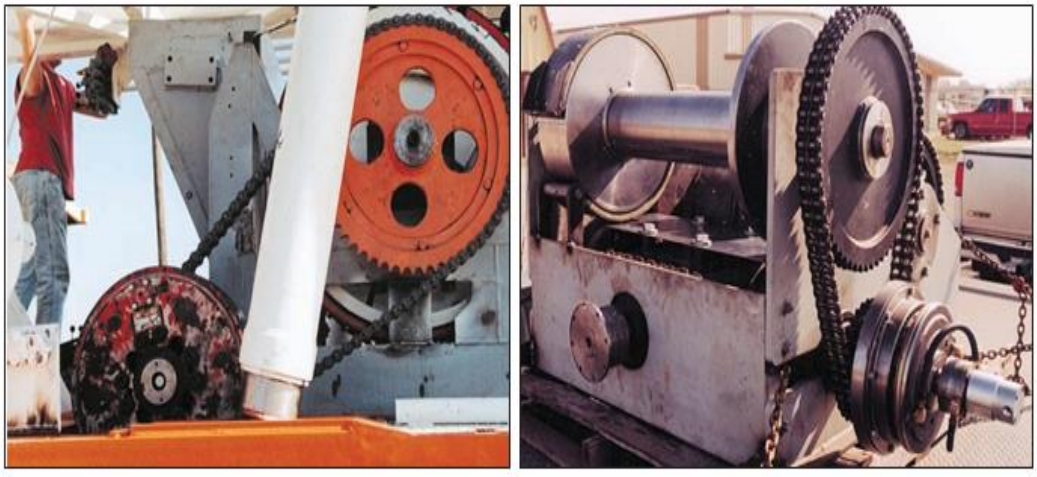

Figure 8: Chains[7]

Drive shaft	Driven shaft	distance between centres	Step	sprocket		Gear wheel		l_m
				Z_1	D_1	Z_2	D_2	
Engines	**Input shaft**	**52.59**	**$1''\frac{1}{2} - 3$**	**28**	**13.39**	**51**	**24.36**	**110**
Input shaft	**Output shaft HI**	**23.930**	**2''-3**	**19**	**12.15**	**25**	**15.95**	**46**
Output shaft	**Output shaft L**	**23.93**	**2''-3**	**20**	**12.78**	**42**	**26.76**	**56**
Output shaft	**Drum shaft hi**	**41.95**	**2''-3**	**37**	**23.58**	**43**	**27.39**	**82**
Drum shaft	**Drum shaft lo**	**41.95**	**2''-3**	**19**	**12.15**	**83**	**52.85**	**98**
Drum shaft	**Rotary C shaft**	**47.96**	**2''-2**	**43**	**27.39**	**37**	**23.58**	**88**
Drum shaft	**Cathead shaft**	**51.68**	**2''-1**	**39**	**24.85**	**21**	**13.41**	**82**

l_m: number of chain links.

Z: number of teeth of the gears.

values in inches.

II.4.3. Clutch's:

- **Mechanical clutch:** features a pressure plate and one or more friction (fibre) plates. Mechanically inserting a cone into the pressure assembly will put great pressure on the friction plates. Internal springs allow for release, allowing the plates to be separated. Segmented plates are used by some contractors for simple installation. However, any clutch that uses segmented plates will be noisy and make a clattering sound when disengaged, especially at low rpms, as in a drawworks, despite the fact that replacement is quick. The kind of cone must be used with extreme caution. It must be a nonlocking cone in the drawworks. To put it another way, it cannot lock the clutch out of center, as would be necessary if it were being used as a line clutch for a pump or compressor. a locking cone in

a drawworks will spook the driller, run the block into the crown, break the line, cause lots of damage, and possibly harm workers.

- **Mechanical positive:** Some drawworks use a jaw clutch or a pin-type clutch. These can be used in conjunction with a master clutch. Of course, these clutches do not slip, and particular attention must be given so that only one of possibly three clutches is engaged

- **Air clutches diaphragm type:** the mechanical clutch's pressure group has been swapped out for an air chamber that can expand between two rigidly attached plates. Literally speaking, 100 psi is equal to 100 pounds of pressure per square inch. These costs add up quickly, and typically a clutch of a much lower size can be chosen to achieve the same torque rating as the mechanical clutch.

- **Air clutches tube type:** Again, the same as previously mentioned, with the exception that the air chamber now resembles a continuous flat vehicle inner tube in many ways. The tube's restricted trip will be expanded by inflation, providing pressure to the plates. clutch tube after the job is deemed safe. All of the aforementioned clutches now include steel separator plates with internal splines fitting on the clutch hub and backplate, as well as friction plates with external splines fitting in the driving ring.

- **Air clutches tube type drum type friction surface:** Clutch plates, splines, and drive rings are not present in this entirely unique design. Typically, a cast iron drum serves as the friction surface. The best friction coefficient for brake and clutch shoes or bands is provided

  by cast iron. The pressure group consists of a steel rim with friction shoes mounted internally and a flat air tube mounted internally. [7].

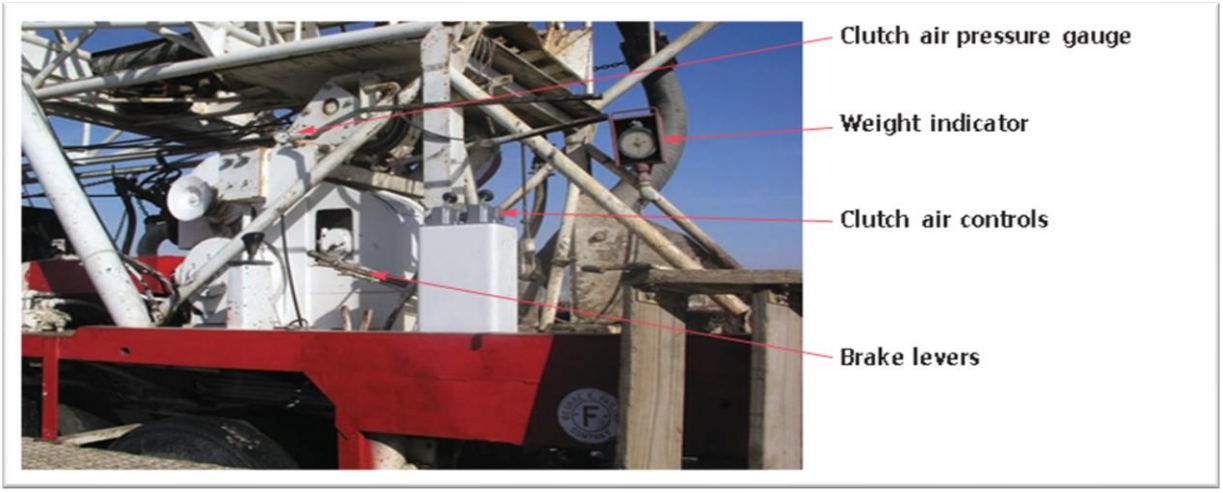

Figure 9 : Drawworks [7]

II.5. Braking system:

II.5.1. Main brake:

II.5.1.1. Band brake:

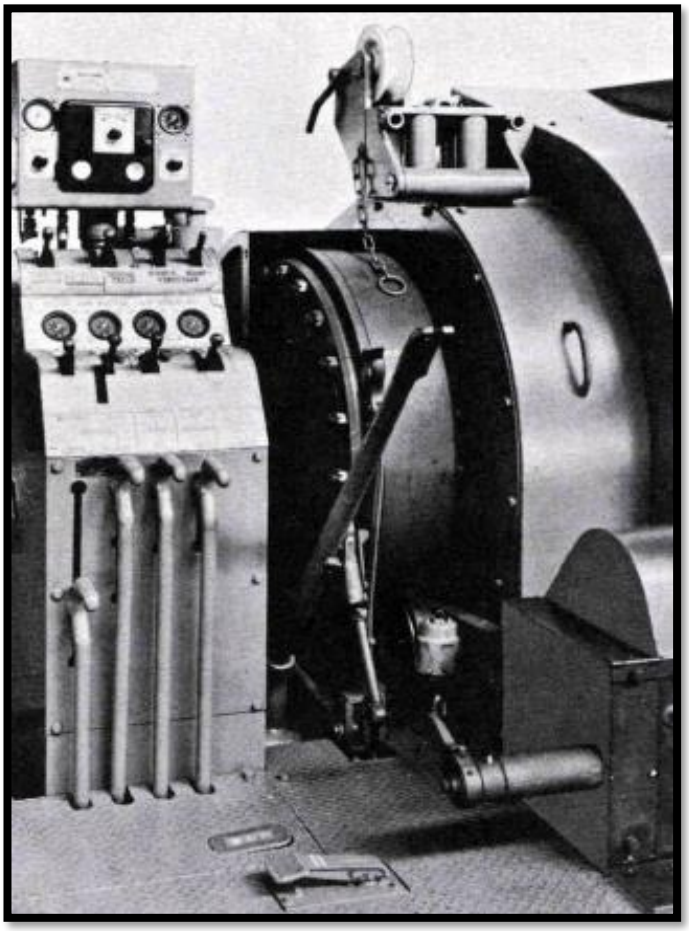

Figure 10: Band brake

The main brake is crucially important to a drilling rig because it slows or stops the drum. It is also called a mechanical brake because it uses only mechanical energy to work. The crew must adjust it, service it, and reline it regularly and should the reform be thoroughly familiar with its construction and operation[1].

The band brake consists of two metalique bands on each side (left band and right band) in a round form, these bands are related by the balanced bar, which splits the braking force into the two bands equally.

it's activated by pushing the Brake handle down towards the floor. Through a strength multiplier system, the braking force is transmitted on the balance bar, then to the brake bands,

and finally to the two drums on either side of main drum. Heat produced by the braking action is dissipated through the circulating water-cooling system.

II.5.1. 2.Disk Brake:

Disk brake systems are commonly used in drawworks to provide reliable and efficient braking. The system comprises a rotating disk, which is mounted on the drawworks shaft, and brake pads that are pressed against the disk to slow down or stop the rotation of the shaft.

The disk itself is typically made of high-strength materials such as steel or cast iron to withstand the high levels of friction and heat generated during braking. It is also designed with channels or grooves to improve the dissipation of heat and reduce the risk of warping or cracking

The brake pads are usually made of friction material such as ceramics, organic compounds, or metallic materials. They are designed to provide high levels of friction against the disk, converting the kinetic energy of the rotating shaft into heat energy, which is then dissipated into the environment. The brake pads are actuated by a hydraulic or pneumatic system, which applies pressure to the pads and causes them to engage with the disk.

To ensure optimal performance, disk brake systems in drawworks require regular maintenance and inspection. This includes checking the wear on the brake pads, ensuring proper alignment of the brake components, and monitoring the levels of hydraulic or pneumatic pressure. Proper maintenance can help extend the lifespan of the brake system and ensure that it operates reliably and safely [3].

Figure 11 : disck brakes

II.5.2. Auxiliary brake / dynamic brake:

The function of the auxiliary brake is to assist the main braking system during rapid descent of the blocks with heavy string weights. The auxiliary brake prevents the overheating and premature wear of main brakes.

There is two Types of auxiliary brakes:

- Hydrodynamic Brake

- Electromagnetic Brake

II.5.2. 1. Hydrodynamic Brake:

consisting of two box with a rotor pressed onto the main drive shaft and two stators. When the main shaft rotates the rotor drags water against the two stators, producing a braking action. Braking capability can be regulated by increasing or decreasing the water levels in the "Hydraulic Brake box".

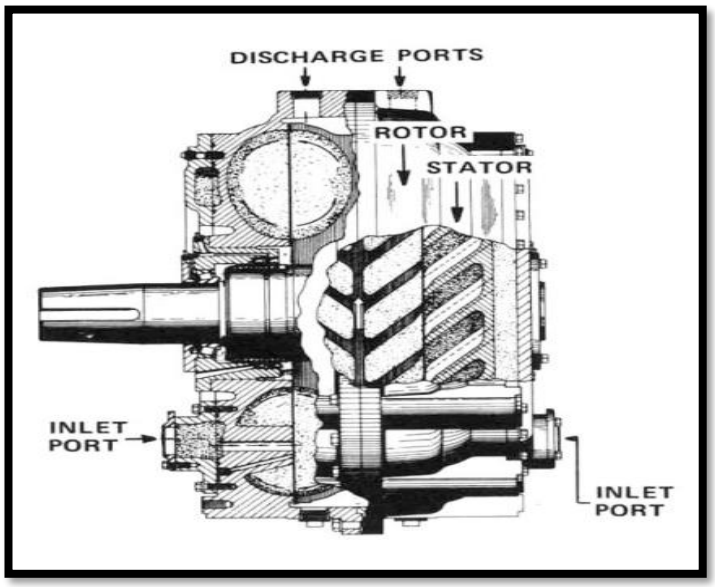

Figure12: Schematic hydrodynamic brake

That system is still in use on small drawworks. However, on medium-Hi powered drawworks, this system has been replaced by the Electromagnetic brake.

II.5.2. 2. Electromagnetic brake:

It works in combination with the main brake to slow the rate of descent of the traveling block with a heavy load. It functions only when the block is descending. ensuring that the load descends slowly and smoothly and it lessens wear on the main brake by taking the heavy shock loads (sudden jerking) and continual dead weight off the brake bands., however, to lower the traveling block slowly enough that the mechanical brake alone could stop it, because the electromagnetic brake could fail [1].

The electromagnetic brake consists of a stator with coil, two magnetic poles and a rotor pressed onto the main drive shaft. When the driller activates the brake control, a magnetic field is produced by 4 electromagnetic coils mounted concentrically inside the drum. By varying the amount of current to these stationery coils, the driller can control the amount of braking torque applied to the rotating drum.

Figure13: electromagnetic brake

II.6. Twin stop system:

is a type of braking system used in drawworks, it consists of two separate braking systems that work in tandem to control the movement of the drawworks and ensure safety during operations.

The Twin stop system is designed with safety in mind and is equipped with an emergency stopping function that can quickly bring the drawworks to a complete stop in case of an emergency. This system is critical in preventing accidents and injuries and can be the difference between a safe operation and a catastrophic failure. Overall, the Twin stop system is a reliable and effective braking system that provides redundancy and safety in drawworks operations. Its ability to provide backup braking force and emergency stopping functions makes it a crucial component in the oil and gas industry.

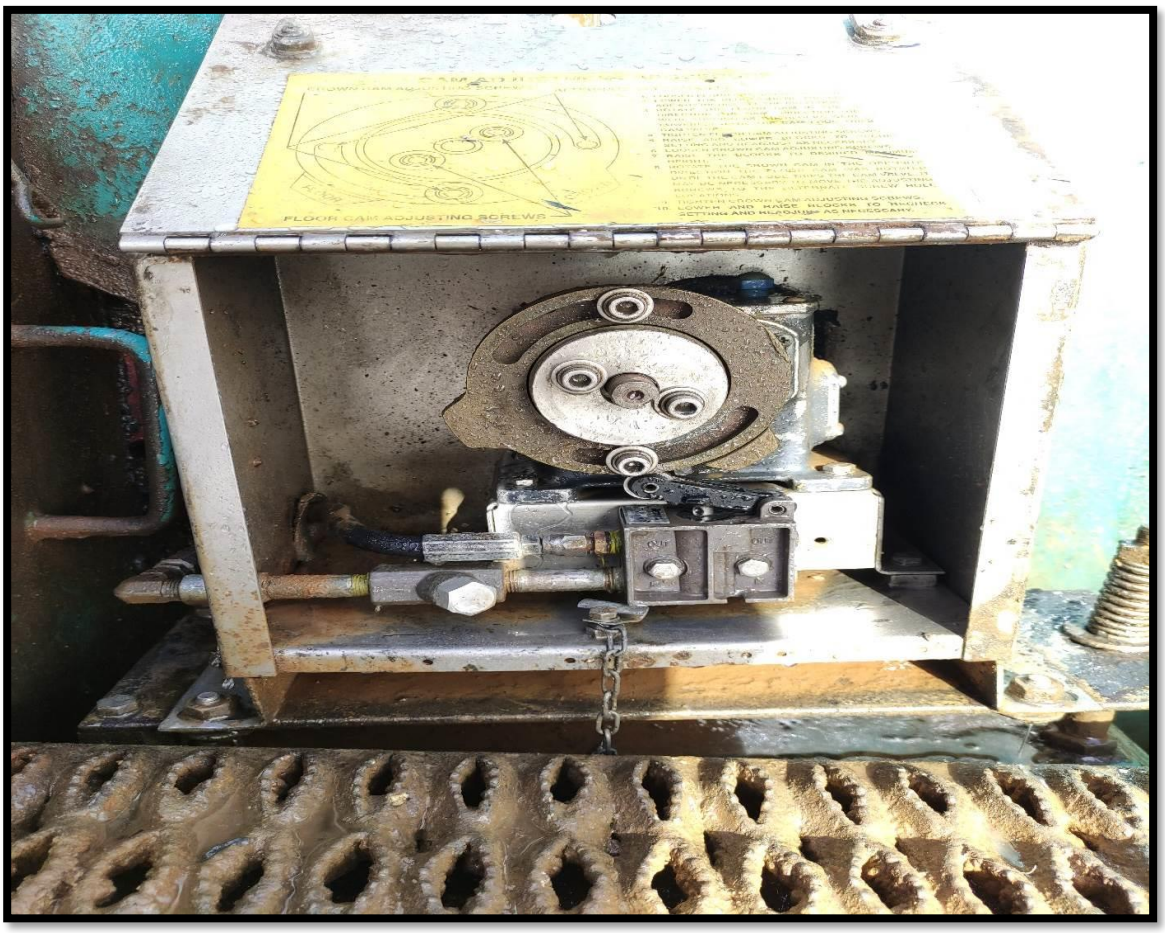

Figure 14: twin stop caliber

II.7. Lubrication system:

Every place on the drawworks were metal rubs against metal needs lubrication. Good lubrication helps the equipment to last as long as possible before breaking. Not only does this mean less expense for replacement parts, but it also means that there is less time when the rig is not drilling because of repairs. Every tour, the operator provides a certain amount of time for inspecting and servicing the rig. The driller keeps a maintenance record, called a tour report, that includes, for example, when the crew measured oil levels, changed oil, checked oil pressure gauges, serviced and replaced filters, and greased fittings. Some parts of the drawworks, such as the transmission, need oil lubrication and some parts need grease[1].

So that means that enough lubrification is very important and required for the movement of mechanical parts also it influence the service life and transmission efficiency, in order to get long, trouble free life drawworks.

Basically, there is two types of lubrification:

- oil lubrification.
- grease lubrification.

Figure 15: lubrification tubes

II.8. Cooling system :

The cooling system typically consists of a network of pipes and a cooling medium, such as water or air, that circulates through the system. As the cooling medium flows through the pipes, it absorbs heat from the braking system and carries it away from the drawworks. This process helps to maintain the temperature within safe operating limits, preventing damage to the braking system and other critical components.

The cooling system is designed to be efficient and reliable, using advanced technologies such as heat exchangers and radiators to transfer heat away from the braking system. The system is also equipped with sensors and controls that monitor the temperature and regulate the flow of the cooling medium to ensure optimal performance**.**[5].

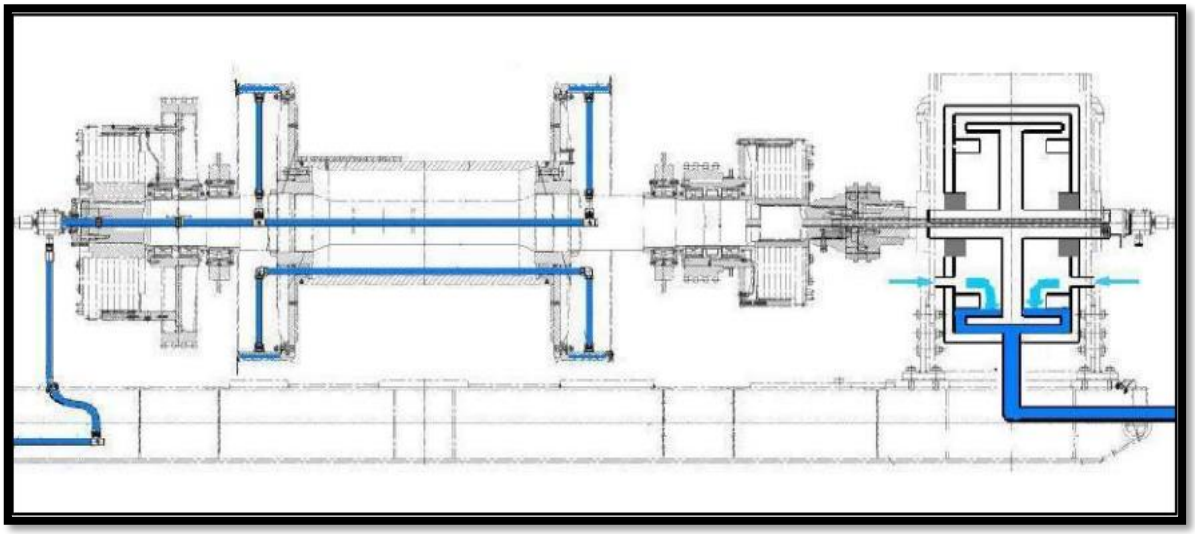

Figure16 : Schematic cooling system[8]

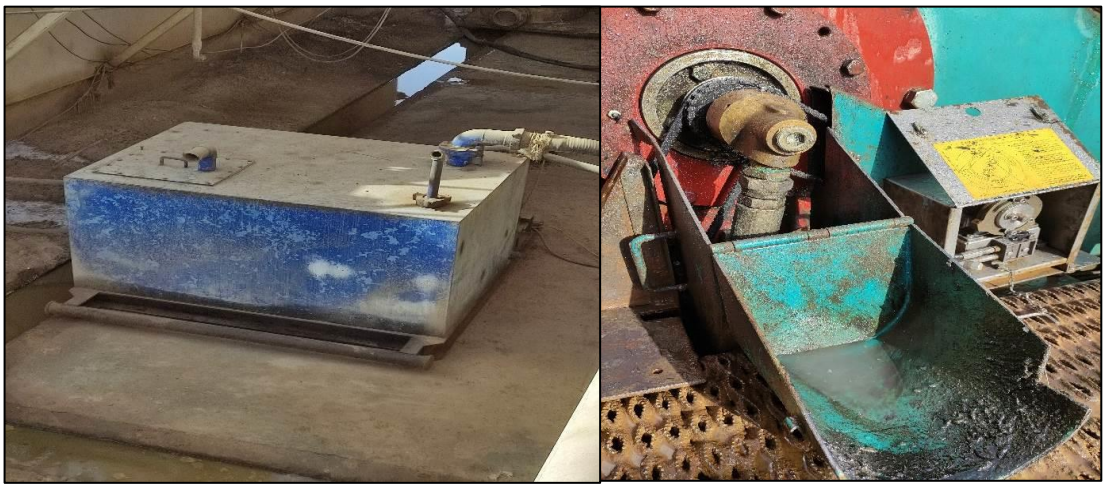

Figure17 – 18: water back – stuffing box

II.9. Catheads:

This system is an important component used in the drilling process for running and retrieving drill pipe, casing, and other drilling equipment. The cathead system consists of a pair of powered drum hoists located on the drawworks, which are used to move drilling equipment into and out of the wellbore. It typically consists of a cable, winch, and drum, which are used to control the movement of the drilling equipment. The cable is wound around the drum, and the winch is used to control the tension and speed of the cable as it moves in and out of the wellbore. The system is designed to be efficient and reliable, with advanced control systems that allow for precise control of the movement of the drilling equipment.

The system is also used to handle other equipment such as blowout preventers, top drives, and other specialized drilling tools.

Overall, the cathead system is a critical component of a drawworks that is essential for efficient and safe drilling operations. By providing precise control of the movement of drilling equipment, it ensure the safety of personnel and prevent damage to equipment, reducing downtime and maintenance costs[3].

Figure 19: cathead

III. Heat exchangers:

Heat exchangers are used to transfer heat between two sources. The exchange can take place between a process stream and a utility stream (cold water, pressurized steam, etc), a process stream and a power source (electric heat), or between two process streams resulting in energy integration and reduction of external heat sources. Typically, a heat exchanger is used with two process streams. However, multi stream heat exchangers are sometimes used with energy extensive processes, to reduce capital cost. The term heat exchanger applies to all equipment used to transfer heat between two streams. However, the term is commonly used to equipment in which two process streams exchange heat with each other. In the other hand, the term heater or cooler is used when the exchange occurs between a process stream and a plant service stream. Other terms used to describe heating equipment include: vaporizer and reboiler (for vaporization) and evaporator (for stream concentration). Exchangers can also be classified as fired (heat source is fuel combustion) and unfired exchangers. There are many types of heat exchangers applied in the process industry. These types include:

1. Hairpin/Double pipe exchangers
2. Shell and tube exchangers
3. Plate and frame exchangers
4. Plate-fin exchangers
5. Spiral heat exchangers
6. Air coolers and condensers
7. Direct contact (quenching towers)
8. Fired heaters

The selection of a heat exchanger depends on many factors including capital and operating costs, fouling, corrosion tendency, pressure drop, temperature ranges, and safety issues (tolerance to leakage). Different types of heat exchangers are shown in Figure 42. In process calculations, the main objectives of heat exchanger calculations are to determine the heat duty (amount of energy to be transferred), temperature changes within the exchanger, and pressure drops. Depending on the degree of details available/needed, the calculations might be simple or thorough.

III.1. Earth-water heat exchanger:

Soil is considered to be a very important heat potential that can be used in many fields. The recovery of thermal energy from the ground is basically performed through a network of water/ground type underground heat exchangers. This is a system for circulating water in pipes that go underground at a certain depth. The temperature in the basement changes less than the outside air, so the water can be cooled or heated depending on the temperature difference between the ground and the water. When water cools, heat transfers to the ground, but when water heats up, it transfers heat according to the first law of thermodynamics.

In the OIL field and during summer peak time, cooling load presents about 70% of the overall energy consumption. The need for efficient cooling system pushes engineers to look for innovative cooling solutions [9], in consistence with the sustainable development goals to reduce consumption and utilize renewables, earth water heat exchanger (EWHE) has drawn the interest of different research groups. The Earth's massive thermal capacitance provides a passive mean of heating and cooling[10], as a result the geothermal cooling has been investigated in various regions so they invented different configurations for ground heat exchangers [11], such as the vertical and the horizontal heat exchangers.

Figure 20: earth-water heat exchanger used in a house cooling system

Chapter II

Bibliographic analysis

I. Introduction:

The braking system of drawworks is a crucial component in the drilling industry as it ensures the safety of personnel and equipment during operations. however, the traditional braking systems are associated with high energy consumption, resulting in increased operational costs and environmental impact. As a result, there has been a growing interest in developing innovative and sustainable braking systems that address these challenges. One such solution is the use of earth to water heat exchangers to enhance the efficiency of the braking system.

The application of earth to water heat exchangers in drawworks braking systems is a relatively new concept that has gained traction in recent years. This technology involves using the stable temperature of the earth to transfer heat between the drawworks and the ground, improving the performance and efficiency of the braking system. This innovative solution has the potential to not only reduce energy consumption and operating costs but also enhance the safety and reliability of the braking system.

As the interest in this technology continues to grow, there is a need for bibliographic analysis to explore the current state of research in this area. Such an analysis will provide a comprehensive understanding of the existing literature, including the key findings, trends, and research gaps. This information can be used to identify areas for further research and development, leading to the continued advancement of drawworks braking systems using earth to water heat exchangers.

II. Bibliographic analysis:

Dakhil and Hammadi's.[12] ANSYS 20/FLUENT software-based investigation focused on the effectiveness of earth-water heat exchangers (EWHE) in hot climate regions. They highlighted the critical role of water storage tanks in water supply systems for commercial and residential buildings. However, the installation of tanks on rooftops in gravity-fed buildings presents a challenge during the hot summer months in Iraq. To address this, an earth-water heat exchanger was proposed, consisting of buried pipes installed underground to reduce the water temperature in the storage tank. The study utilized experimentally and theoretically analysing for both the storage tank and EWHE to estimate the water temperature. Using a pipe length, diameter, and mass flow rate of 100 m, 0.016 m, and 0.7 LPM, respectively, at a depth of 3 m resulted in a 15 °C reduction in water temperature. The

research highlights that utilizing an earth-water heat exchanger can effectively decrease the temperature of stored water in hot climate regions, making it suitable for cooling purposes.

Atwany et al.[13] conducted two experimental studies to evaluate the effectiveness of ground heat exchangers(GHE) in Sharjah, United Arab Emirates. The first study focused on the ground temperature distribution for two boreholes, each with a depth of 10 meters, over seven months. The results showed that the temperature was 5 degrees higher than the average ambient temperature for the year. In the second study, the performance of a GHE was examined under Sharjah city conditions. The GHE was made up of a 300-meter-long plastic pipe with a diameter of 0.03 meters, buried horizontally at a depth of 2.5 meters below the ground surface. The results indicated that the GHE increased ground temperature and required approximately 9 hours to disperse thermal energy. The study also found that a mass flow rate of 0.15 kg/s produced greater heat exchange and GHE efficacy compared to a lower flow rate of 0.0375 kg/s. However, the effectiveness of the GHE decreased over time, and this decrease was more significant as the mass flow rate increased.

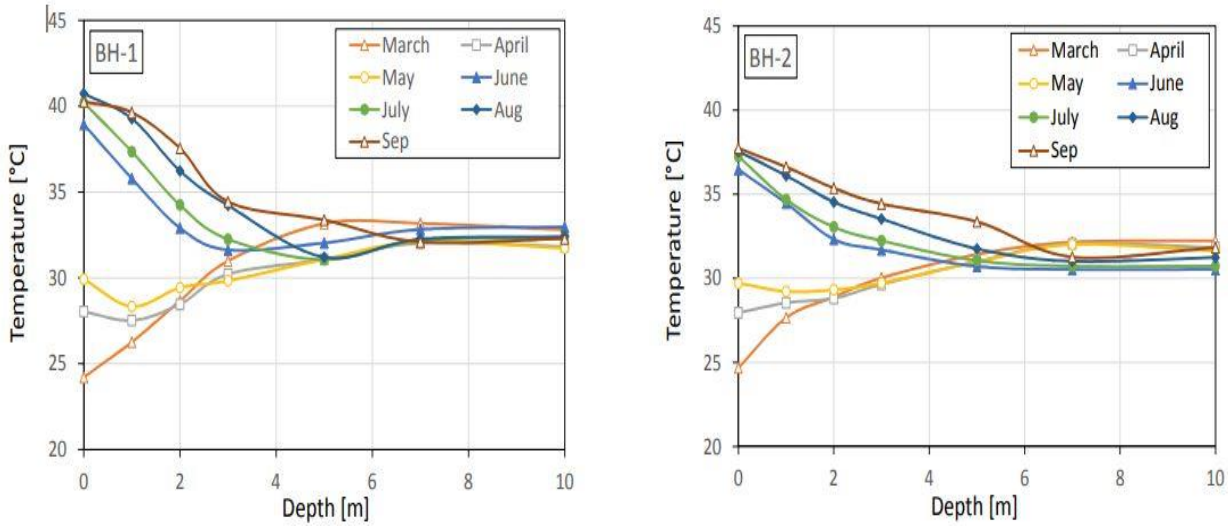

Figure 1: Ground temperature distribution at borehole 1 and 2 (BH-1-2).

Atwany et al.[9] studied the thermal effectiveness of a horizontal EWHE designed for cooling applications. Using ANSYS Fluent software, they developed a two-dimensional model and analysed how factors such as inlet water temperature, velocity, soil thermal conductivity, and ground surface temperature affect heat transfer rates. The findings indicated that higher soil thermal conductivity led to increased heat transfer, while lower ground surface temperature resulted in better heat exchange rates.

Elminshawy et al.[14] assessed the effectiveness of a buried water heat exchanger (BWHE) cooling system integrated with a V-trough PV concentrator. A specialized test rig was constructed and tested in Port Said, Egypt. The study analysed the impact of varying cooling water flow rates ranging from 0.01 kg/s to 0.04 kg/s on the performance of the system. The cooling system employing a BWHE successfully reduced the maximum panel surface temperature from 72.5°C without cooling to 47.2°C, 45.5°C, 41.8°C, and 39.3°C at water cooling flow rates of 0.01 kg/s, 0.02 kg/s, 0.03 kg/s, and 0.04 kg/s, respectively. Additionally, the generated electrical power (GEP) peak increased by 18.6%, 20.9%, 23.5%, and 28.3% compared to the uncooled panel at water cooling flow rates of 0.01 kg/s, 0.02 kg/s, 0.03 kg/s, and 0.04 kg/s, respectively. The electrical and thermal efficiencies improved with increasing cooling water flow rates. An economic evaluation was conducted to determine the unit price of power, and the results demonstrated that the proposed cooling system reduced the relative levelized cost of energy by 12.20%, leading to a decrease in global average CO2 emissions of roughly 49,209 g CO2/summer season.

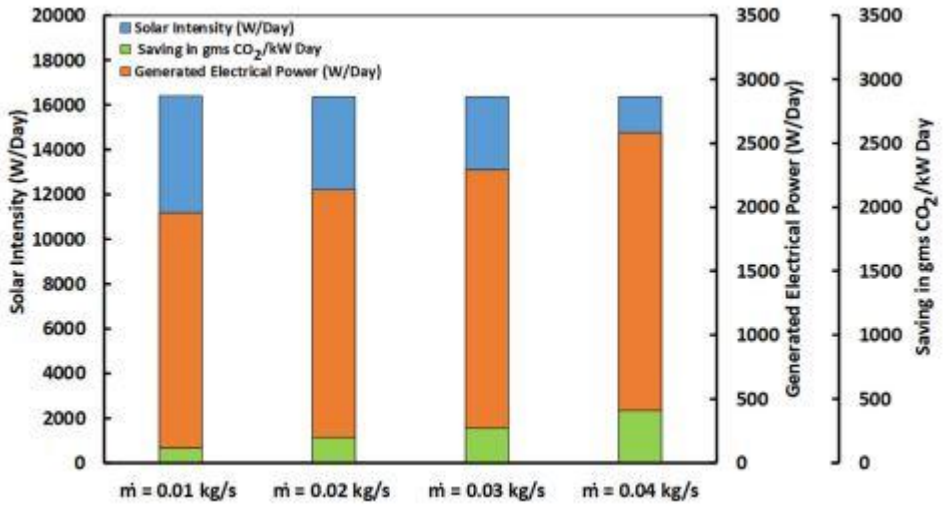

Figure 2: The daily accumulated solar intensity, the decrease in CO2 due to using geothermal cooling and the generated electrical power for different geothermal cooling water flow rates.

Salman H. Hammadi.[15] discussed the use of an EWHE as a means of reducing the temperature of water storage tanks in hot climates. Explaining that in regions with high ambient temperatures, water stored in tanks can reach high temperatures, leading to energy waste and reduced water quality. The study proposes using an EWHE system, which involves burying a plastic pipe in the ground and circulating water through it before entering the tank. The experimental testing of the EWHE system in the United Arab Emirates reported that the system was able to reduce water temperature by as much as 14°C, leading to improved water quality and reduced energy consumption.

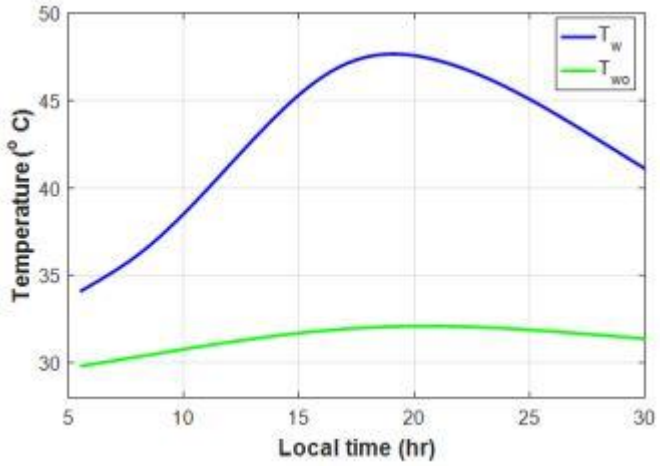

Figure 3: daily temperature profile of tank water and outlet water of EWHE in august

Mohammad O, Hamdan.[16] explored the design of a highly effective EWHE To capture geothermal energy. The study utilized numerical simulations to evaluate the thermal performance of the EWHE system under different operating conditions. The results of the study revealed that the EWHE system can efficiently extract geothermal energy, providing significant heating and cooling benefits. The system showed a maximum temperature difference of 20°C between inlet and outlet water temperatures, with a heat transfer rate of 0.89 kW. The findings suggest that the EWHE system could be a promising and efficient alternative to traditional heating and cooling systems, especially in regions with high geothermal potential.

Kappler et al.[17] Made an investigation that was conducted to evaluate the effectiveness of using soil as a heat source and sink, along with buried water tanks as thermal accumulators. The study involved the construction of an experimental prototype to assess heat exchange between the tank and soil, with data obtained used to estimate the performance of a real-scale water tank. Heating and cooling power outputs were calculated using 'EnergyPlus' software to determine power requirements for maintaining building temperatures at 18°C in winter and 25°C in summer. The study found a maximum heat exchange rate of 24.66 kWh/day, suggesting

that the proposed technique is a reliable option for natural air conditioning of buildings and can overcome constraints of traditional ground heat exchange systems.

Atwany et al.[18] aimed to understand the heat flow in the EWHE by analysing the thermal conductivity of soil as a function of various parameters. Samples were collected from the American University of Sharjah Campus at a depth of 2 meters below ground level, and their thermal conductivity was measured using a C-Therm Technologies analyser. The study revealed that the thermal conductivity of soil increases with an increase in water content and dry density. However, the initial water content has a more significant effect on thermal conductivity than the initial dry density. The study also found that porosity affects the hydraulic conductivity of the sand.

T. Sivasakthivel et al.[19] Experimentally investigated the thermal performance of ground heat exchangers for space heating and cooling applications. The study was conducted using a test rig consisting of a GHE, a heat pump unit, and a water tank. The thermal performance of the GHE was evaluated under different operating conditions, including heat pump capacity, flow rate, and soil moisture content. The results showed that the GHE was capable of extracting heat from the ground during the winter and rejecting heat to the ground during the summer, with an average thermal efficiency of 3.3. The study also found that increasing the heat pump capacity and flow rate can improve the thermal performance of the GHE, while increasing the soil moisture content can have a negative effect on the system's performance. Overall, the study provides valuable insights into the design and operation of GHE systems for space heating and cooling applications.

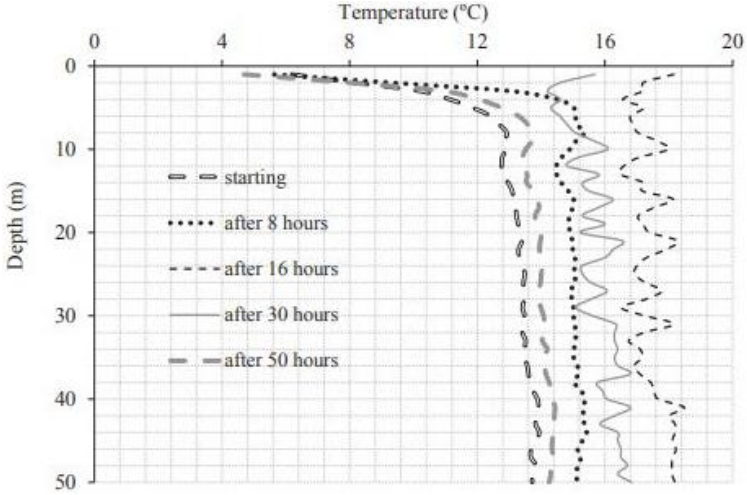

Figure 4: Double U-tube - ground temperature variations - cooling.

Jun Kim et al.[20] Focused on the thermal performance evaluation and parametric study of a horizontal GHE for ground-source heat pump (GSHP) systems. The study used a 2D numerical model to simulate heat transfer processes in the GHE under different operating conditions. The results indicated that the thermal performance of the GHE is affected by factors such as pipe spacing, diameter, and depth, as well as soil thermal conductivity and inlet fluid temperature. The study found that decreasing pipe spacing and increasing pipe diameter and depth can improve the thermal performance of the GHE. Additionally, it was found that increasing soil thermal conductivity can lead to higher heat transfer rates. The findings of this study provide valuable insights for the design and optimization of horizontal GHE systems for GSHP applications.

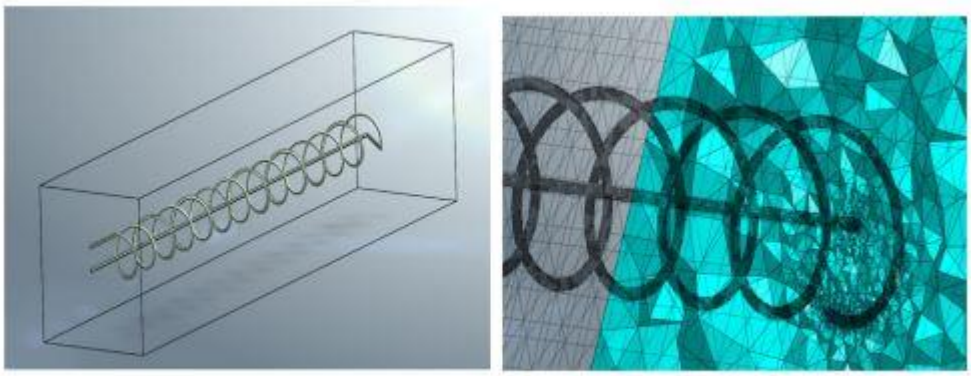

(a) Finite element model (b) Mesh formed in the program

Figure 5: Finite element model for the numerical simulation

Jakhar et al.[21] discussed the performance analysis of an EWHE system for cooling a Concentrating Photovoltaic (CPV) module. The study utilized numerical simulations to investigate the thermal performance of the EWHE system under various operating conditions. The results indicated that the EWHE system can effectively reduce the temperature of the CPV module and provide significant cooling benefits. The system demonstrated a maximum temperature difference of 27°C between the inlet and outlet water temperatures, with a heat transfer rate of 1.3 kW. The findings suggest that the EWHE system can be a promising and efficient alternative to conventional cooling systems for CPV modules.

Table 1. Applicability of EWHE system with existing literature[22, 23].

Author	Concentration ratio (CR) (Suns)	CPV cells material	Flow rate (kg/s)	Water outlet temp. from CPV/T (EWHE Inlet) °C	Water outlet temp. from EWHE (CPV/T inlet) °C	Pipe length required for EWHE (meter)
Xu et al. -2012	**50 (Straight)**	**Monocrystalline silicon**	**0.00045**	**58.7**	**24.2**	**5**
	50 (Tree)		**0.00044**	**55**	**24.3**	**4**
Li et al. (2011)	**16.92**	**CS and PS**	**0.012**	**48.5**	**25.5**	**60**
	16.92	**SCA**	**0.012**	**47**	**25.7**	**58**
	16.92	**GaAs**	**0.012**	**42.5**	**26**	**52**

Sivasakthivel et al.[24] experimentally studied a ground source heat pump (GSHP) system installed in a Himalayan city in India. The study aimed to evaluate the thermal performance of the system under composite climatic conditions. The GSHP system consists of a horizontal ground heat exchanger, a water-to-water heat pump, and a thermal energy storage tank. The study involved monitoring the system's performance over a year, including its coefficient of performance (COP) and energy consumption. The results showed that the system had an average COP of 3.3 and consumed 22.9 kWh of energy per day. It also evaluated the system's performance under different operating conditions and found that the COP varied between 2.6 and 3.9, depending on the ambient temperature and the heat load. Overall, the study concludes that the GSHP system can be an efficient and sustainable alternative to conventional heating and cooling systems in the Himalayan region of India.

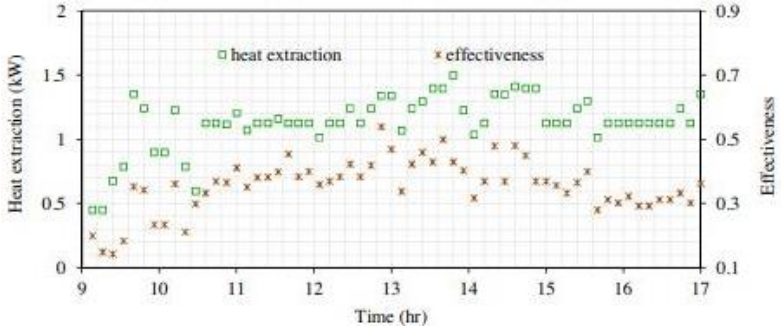

Figure 6: Heat extraction and effectiveness

Rouag et al.[25] discussed the proposal of a supplementary cooler that utilizes an EWHE to improve the performance of a solar adsorption cooling machine (SACM) in semi-arid regions. The study analyzed the performance of the SACM with and without the EWHE using simulation models and experimental measurements. The results showed that the SACM with the EWHE had a higher cooling capacity and COP compared to the SACM without the EWHE. The study concludes that the proposed system has great potential for providing sustainable and cost-effective cooling solutions in semi-arid regions with high solar radiation.

Serageldin et al.[26] investigated the impact of groundwater flow on the thermal performance of a novel borehole heat exchangers for Ground source heat pump systems. The research conducted small-scale experiments to measure the temperature distribution around the BHE and the heat transfer rate under different groundwater flow conditions. They also developed a numerical simulation model to predict the thermal performance of the BHE under various operating conditions. The study found that groundwater flow has a significant impact on the thermal performance of BHEs, with increased flow rates leading to reduced heat transfer rates and thermal interference between adjacent boreholes. The numerical simulation model provided accurate predictions of the temperature distribution and heat transfer rates of the BHE under different operating conditions, confirming the experimental results. The findings of this study are important for the development and optimization of BHEs for GSHP systems. By understanding the impact of groundwater flow on BHE performance, designers and operators can make informed decisions and implement measures to ensure optimal system performance, leading to increased energy efficiency and reduced carbon emissions.

Yang et al.[27] investigated the use of a cooling system that utilizes shallow-geothermal energy to address the issue of declining photovoltaic panel conversion efficiency. The system cools the panels by spraying water onto the back of the panels and then returns the water to a tank. To increase the cooling capacity, the recycled water is circulated through a U-shaped borehole heat exchanger (UBHE), which exchanges heat with shallow-geothermal energy. The panel is then cooled again by spraying it with water. The study involved three stages: operating the panel without a cooling system, operating it with a cooling system but without a UBHE, and operating the cooling system with a UBHE. Both the experimental results and the mathematical model show that the cooling system can significantly improve the panel conversion efficiency,

particularly as the temperatures and number of panels increase. For a plant factory powered by panels, the cooling system can improve the efficiency by 14.3%. The equipment costs of the cooling system can be recovered within 8.7 to 22 years, depending on the specific implementation.

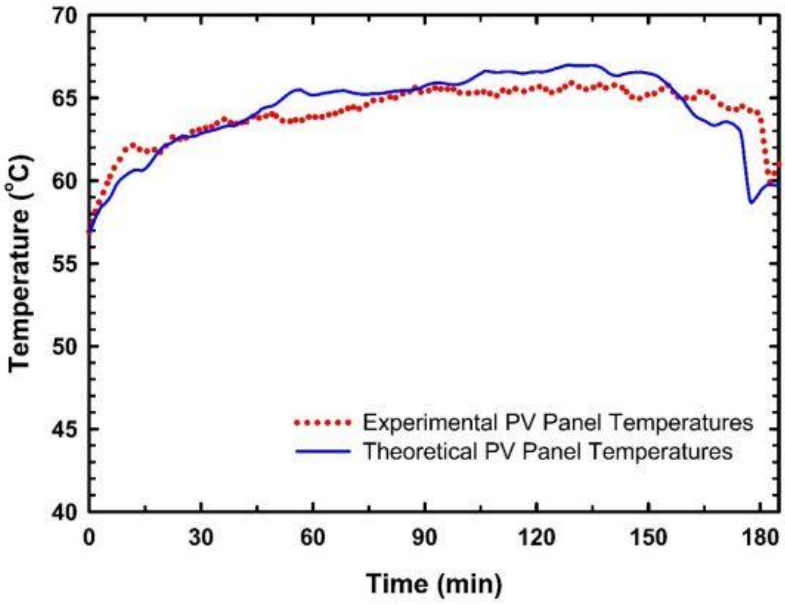

Figure 7: Relationship between the PV panel temperatures and the cooling water temperatures (experimental results and theoretical predictions)

Choudhary et al.[28] discusses a comparative life cycle assessment of different photovoltaic thermal (PVT) systems with and without earth water heat exchanger cooling (EWHEC). The study aimed to evaluate the environmental impact and energy performance of these systems. The results of the study showed that PVT systems with EWHEC had a lower environmental impact than those without it. This was because EWHEC reduced the electricity consumption required for cooling, which in turn reduced greenhouse gas emissions. Additionally, the use of PVT systems with EWHEC resulted in a higher energy yield and a lower cost of energy production compared to PVT systems without it. The obtains concludes that PVT systems with EWHEC are a more sustainable and cost-effective option for renewable energy production compared to PVT systems without it. It also highlights the importance of considering the environmental impact of renewable energy systems throughout their entire life cycle, from raw material extraction to disposal.

Jakhar et al.[29] aimed to analyse the energy and exergy performance of the system and investigate the effect of different parameters on its performance. The study found that the integrated photovoltaic thermal solar system with EWHEC had a higher thermal efficiency and electricity generation efficiency compared to a conventional photovoltaic system. The EWHEC system helped to reduce the temperature of the photovoltaic panels, which improved their electrical efficiency. In addition, the system provided a significant amount of thermal energy for space heating or water heating, making it a more efficient use of solar energy. The study also found that the performance of the system was affected by various parameters such as ambient temperature, water flow rate, and collector inclination angle. For instance, increasing the water flow rate resulted in higher thermal and electrical efficiencies, while increasing the collector inclination angle improved the electrical efficiency but decreased the thermal efficiency.

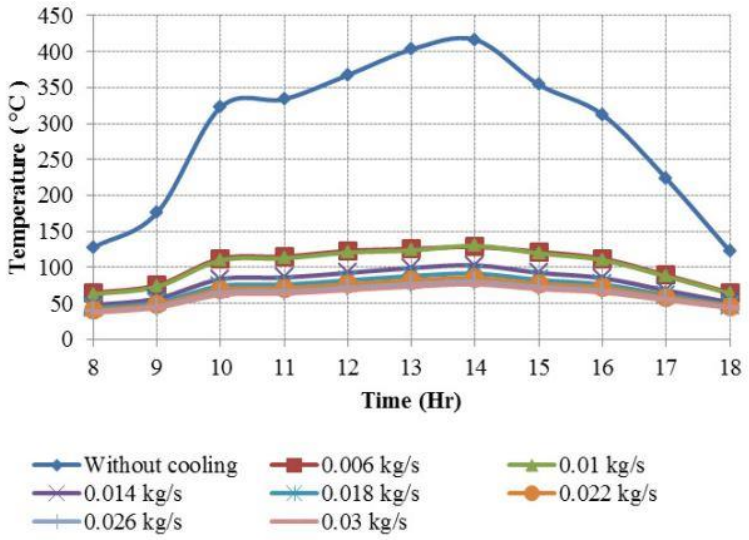

Figure 8: CPV panel temperature with cooling and without cooling for various mass flow rates (Suns=3).

Chao Li et al.[30] investigated the effect of inner pipe type on the heat transfer performance of deep-buried coaxial double-pipe heat exchangers. They compared the thermal performance of two types of inner pipes, a smooth pipe and a spiral pipe, and to determine the optimal inner pipe design for efficient heat transfer. The researchers conducted a series of experiments using a full-scale test rig that simulates the deep-buried coaxial double-pipe heat exchangers with the two different types of inner pipes. The experiments were conducted under different operating conditions, including varying flow rates and temperatures. The results of the study showed that the spiral inner pipe design had better heat transfer performance than the smooth inner pipe design, with a higher overall heat transfer coefficient and a lower thermal resistance. The researchers also found that the optimal design parameters for the spiral inner pipe were a helix angle of 45 degrees and a pitch of 60 mm. The study concludes that the spiral inner pipe design

is more efficient for heat transfer in deep-buried coaxial double-pipe heat exchangers and could offer a more sustainable and cost-effective alternative to traditional heating and cooling systems. The findings of this study could have important implications for the design and optimization of deep-buried coaxial double-pipe heat exchangers.

Jakhar and Manoj S. Soni.[31] presented a study on a hybrid photovoltaic thermal (PVT) system with an earth water heat exchanger cooling system. The performance of the system was evaluated using exergy analysis, which showed that the exergy efficiency of the system increased with increasing air flow rate and decreasing coolant flow rate. The study concluded that the PVT system with an earth water heat exchanger cooling system can provide a high exergy efficiency for both electricity and heat generation, while reducing the cooling load of the building and overall energy consumption.

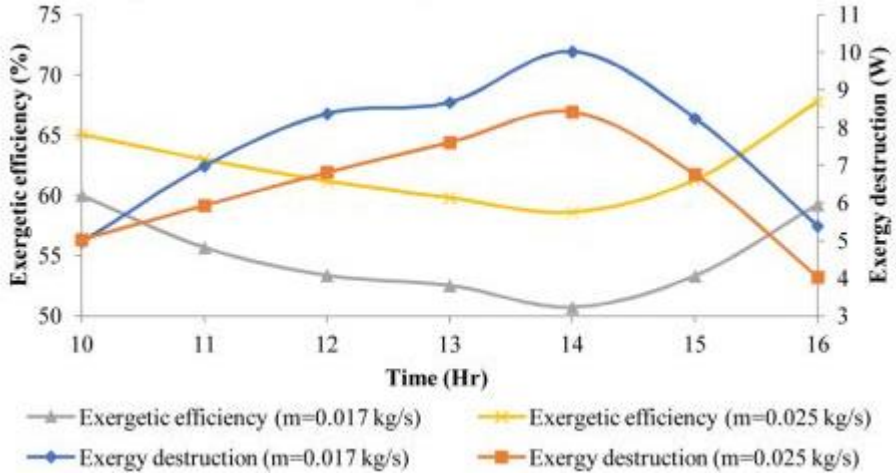

Figure 9: Total exegetic efficiency and exergy destruction of EWHE system for different flow rates

Jakhar et al.[32] presented a comprehensive study on an integrated photovoltaic thermal solar (IPVTS) system with an earth water heat exchanger cooling system. They focused on evaluating the system's energy and exergy performance to determine its efficiency and potential for practical application in building energy systems. The experiments have been conducted using a prototype of the IPVTS system with an earth water heat exchanger cooling system, under various operating conditions, including different flow rates, temperatures, and solar irradiance levels. The energy and exergy analyses were performed to evaluate the performance of the system in terms of electricity and heat generation, as well as the cooling load reduction and overall energy consumption. The results showed that the IPVTS system with the earth water heat exchanger cooling system had high efficiency in electricity and heat generation, with

energy and exergy efficiencies of up to 38.9% and 28.7%, respectively. The system also reduced the cooling load of the building, resulting in lower overall energy consumption. The study suggests that the integration of a photovoltaic thermal system with an earth water heat exchanger cooling system could provide a promising and sustainable solution for energy systems, particularly in hot and humid climates.

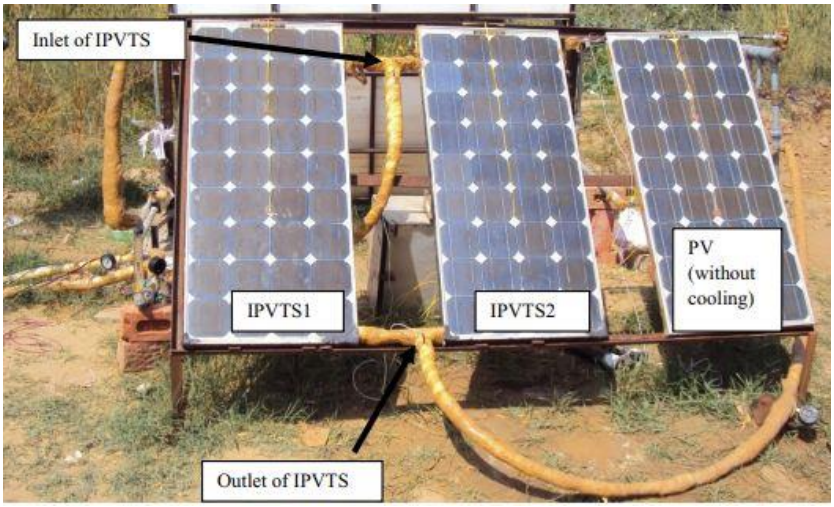

Figure 10: On site experimental setup

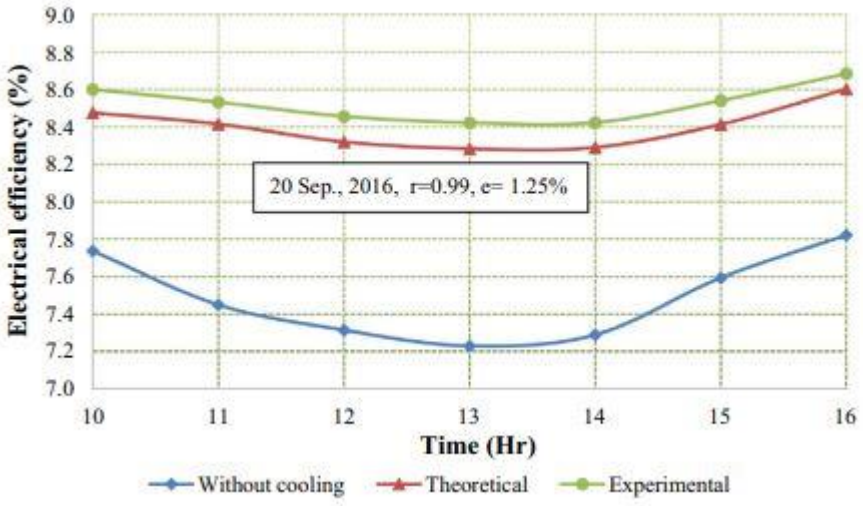

Figure 11: Simulated and experimental values of electrical efficiency of IPVTS during test period.

Yusubov and Aliyev.[33] discussed the temperature distribution in a drilling brake contact, which is an essential component in drilling operations.an experimental studies were conducted to investigate the thermal behavior of the drilling brake contact and the temperature distribution across its surface. They used a thermocouple array to measure the temperatures and analyzed the results to determine the effects of various factors on the temperature distribution, including drilling speed, feed rate, and material properties. The study provides insights into the thermal behavior of the drilling brake contact and could inform the development of more efficient and effective drilling operations.

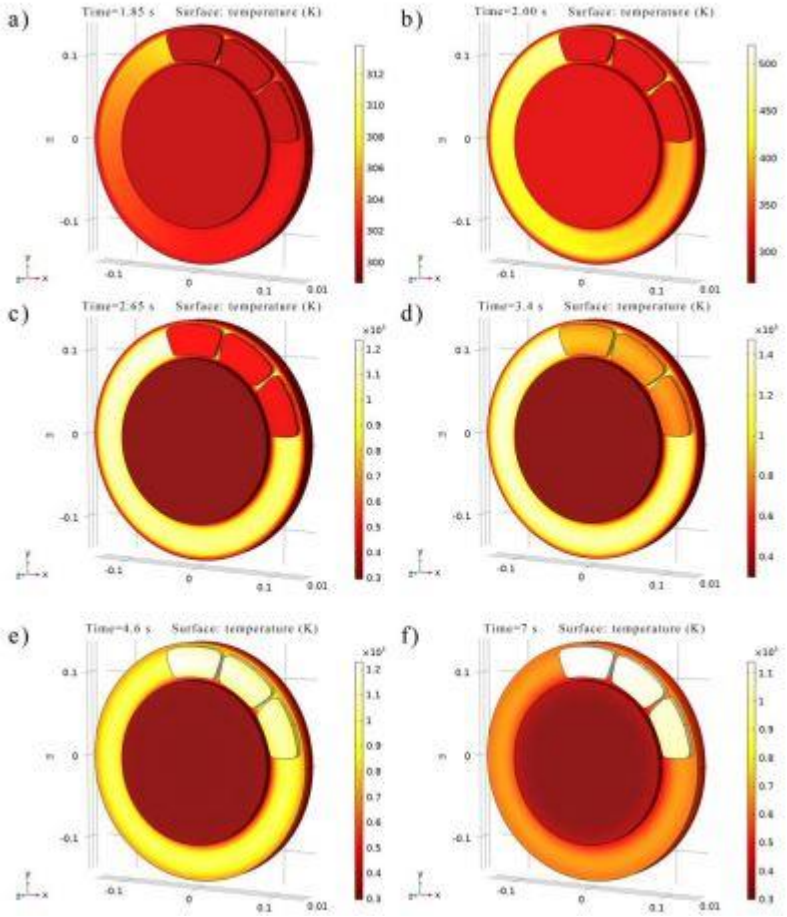

Figure 12: Temperature change during different braking conditions

Chapter III

Mathematical modelling

I. Introduction:

The assessment of the thermal performance of a water-to-ground heat exchanger necessitates the use of suitable thermal models. This chapter presents the development of an analytical model using the general equation of conduction, in steady state, to estimate the temperature distribution of the soil surrounding the exchanger. Moreover, analytical and numerical models in steady-state regime is developed based on the principle of energy balances, to monitor the temperature changes of the water flowing inside the tube. These models enable the evaluation of the thermal performance and efficiency of the water-to-ground heat exchanger.

II. Thermal Model of the Ground:

To extract the maximum amount of cold energy from the first few meters of the subsurface at a reliable cost, it is crucial to determine the optimal depth for placing the water-to-ground heat exchanger in the subsurface. This requires studying the depth of penetration into the ground, where the temperature is either constant or less susceptible to external climatic conditions over time.

II.1. Description and Assumptions:

The soil is assumed to be a uniform and unchanging environment, with consistent properties such as thermal conductivity (λsoil), bulk density (ρsoil), and specific heat capacity (Csol).

The soil moisture's temporal variation resulting from water infiltration is disregarded, and there is no consideration of any groundwater table beneath the heat exchanger's installation area. In the model, the soil is represented as a semi-infinite solid mass.

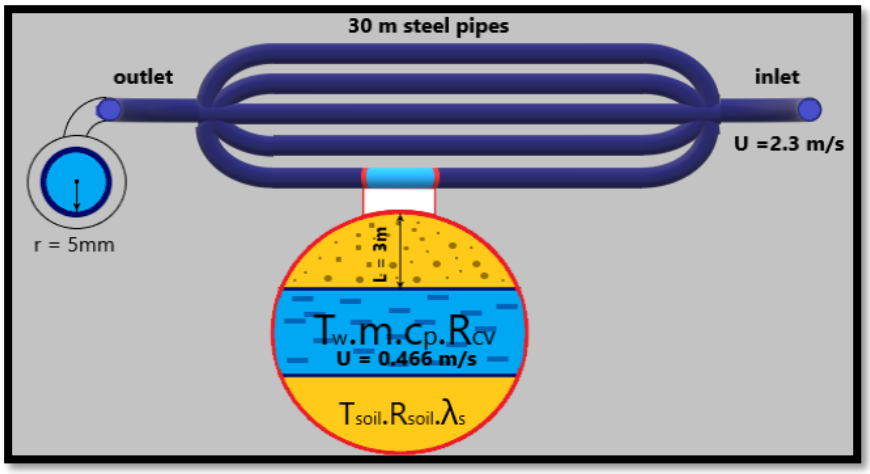

Figure 1: Descriptive diagram of the water/soil heat exchanger.

II.2. Steady-state modelling of soil temperature:

II.1.1. Variable surface temperature of the soil:

The temperature of the soil is governed by the following unidirectional heat equation:

$$\frac{\partial^2 T_{soil}}{\partial z^2} = \frac{1}{\alpha}\frac{\partial T}{\partial t} \quad (1)$$

T: Temperature of the soil in [degrees].

t: Time in [s].

z: Vertical coordinate in [m].

α: Thermal diffusivity of the soil [**α=λ/(ρ.cp)**] (m2/s).

λ: Thermal conductivity of the soil in (w/(m.deg)).

ρ: Mass density (kg/m3).

Cp: Specific heat of the soil in (j/kg.deg).

When the transfer occurs in a steady state, the temperature profile is written as:

$$T_{soil}(z) = a.z + b \quad (2)$$

Where a and b are two integration constants to be determined by the following boundary conditions:

$$\begin{cases} T_{soil}(z=0) = T_{wall} \\ T_{soil}(z=\delta) = T_i \end{cases} \quad (3)$$

Where δ is the burial depth of the exchanger, Ti is the initial temperature of the soil, and Tp is the temperature at the soil wall (Fig.1). To determine the temperature at the soil wall, continuity of heat flew between the soil and ambient water is ensured by the following relation:

$$-\lambda \frac{\partial T_{soil}}{\partial z}\Big|_0 = h(T_{wall} - T_{win}) \quad (4)$$

After integrating equation (4), we obtain:

$$-\lambda \frac{(T_i - T_{wall})}{\delta} = h(T_{wall} - T_{win}) \qquad (5)$$

Where λ is the thermal conductivity of the soil, h is the average convective heat transfer coefficient between the ambient water and the soil, and **T_{win}** is the temperature at the inlet of the exchanger, temperature going out from the brakes.

We obtain the temperature at the surface of the soil **T_{wall}** as follows:

$$T_{wall} = \frac{\lambda}{\lambda - \delta \cdot h} T_i - \frac{\delta \cdot h}{\lambda - \delta \cdot h} T_{win} \qquad (6)$$

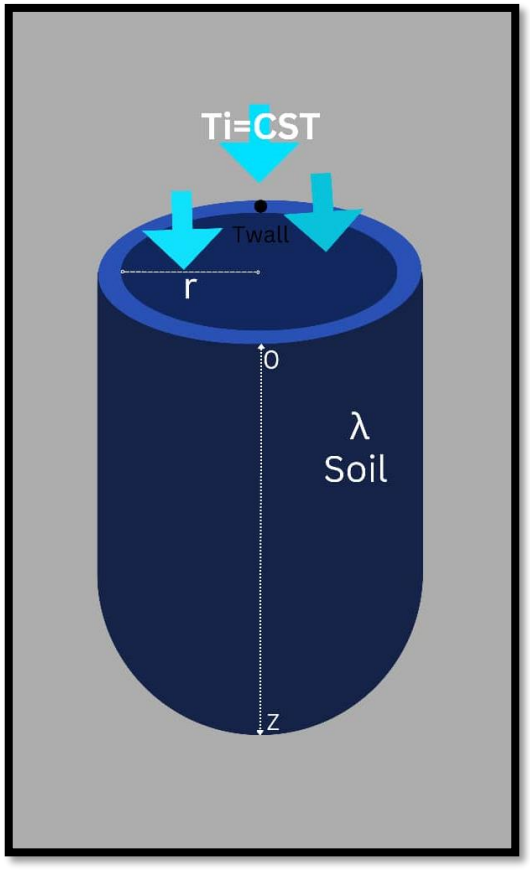

Figure 2: Diagram of the semi-infinite soil medium with constant temperature at the surface.

Therefore, the temperature of the soil away from the exchanger can be written as:

$$\mathrm{T}_{soil}(z) = \frac{T_i - T_{wall}}{\delta} \cdot z + T_{wall} \quad (7)$$

II.3. Transitory modelling of soil temperature:

II.3.1. Variable surface temperature of the soil:

Let us recall the following unidirectional heat conduction equation (1):

$$\frac{\partial^2 T_{soil}}{\partial z^2} = \frac{1}{\alpha}\frac{\partial T}{\partial t} \quad (1)$$

Making the following change of variables:

$$\theta(z,t) = T(z,t) - T_i \quad (8)$$

The equation (1) becomes:

$$\frac{\partial \theta}{\partial t} = \alpha \frac{\partial^2 \theta}{\partial z^2} \quad (9)$$

The boundary conditions to solve equation (3) are explicitly given by equation (10):

- $\theta(\mathrm{z} = 0, \mathrm{t}) = \mathrm{A} \cdot \cos(\mathrm{wt})$
- $\theta(z \to \infty, t) = 0$ (10)
- $\theta(\mathrm{z}, 0) = 0$

Where:

Ti: Average annual temperature at the soil surface, also representing the invariant temperature of the subsoil.

w: Angular frequency [w=2π/365] (rad/day).

A: Amplitude of temperature variation (A=12°C) [°C].

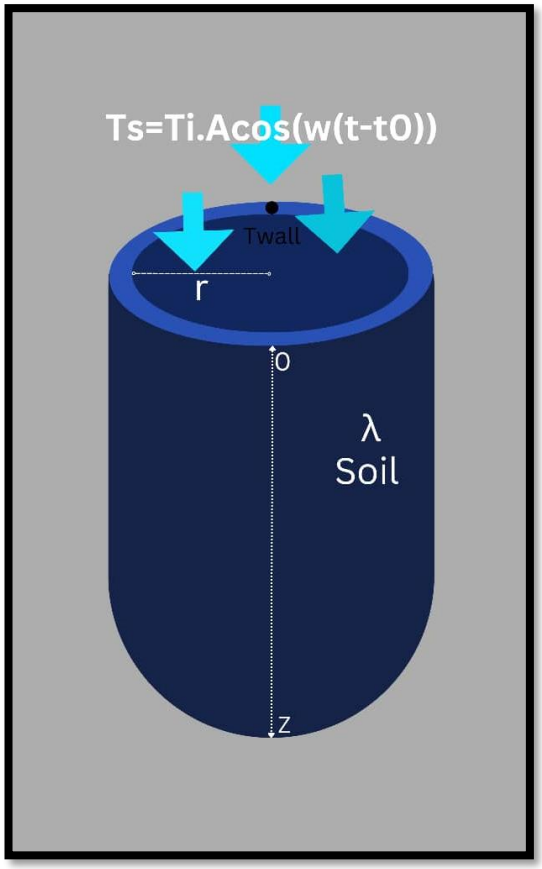

Figure 3: Diagram of the semi-infinite soil medium with variable temperature at the surface.

Using the method of separation of variables to solve equation (9).

$$\theta(z,t) = Z(z) \cdot \tau(t) \qquad (11)$$

Replacing equation (11) into equation (9), we will have:

$$Z(z) \cdot \tau'(t) = \alpha \cdot Z''(z) \cdot \tau(t) \qquad (12)$$

Dividing both sides of the equation by Z(z) * τ (t), we obtain:

$$a\frac{z''(z)}{z(z)} = \frac{\tau'(t)}{\tau(t)} = \beta = \text{ cste} \qquad (13)$$

Where: ß= íw(constant complex number)

From equation (13), we obtain:

$$Z''(z) - \frac{\beta}{a} \cdot Z(z) = 0 \qquad (14)$$

$$\tau'(t) - \beta \cdot \tau(t) = 0 \qquad (15)$$

The solution of equations (14) and (15) will be presented by equations (16) and (17), respectively:

$$Z(z) = a \cdot \exp\left(-\sqrt{\frac{\beta}{a}}z\right) + b \cdot \exp\left(\sqrt{\frac{\beta}{a}}z\right) \qquad (16)$$

$$\tau(t) = c \cdot \exp(\beta t) \qquad (17)$$

The general solution of equation (9) will take the following form:

$$\theta(\mathrm{z},\mathrm{t}) = \left[C_1 \cdot \exp\left(-\sqrt{\frac{\beta}{a}}z\right) + C_2 \cdot \exp\left(\sqrt{\frac{\beta}{a}}z\right)\right] \cdot \exp(\beta t) \quad (18)$$

C1 and C2 are two integration constants, we apply the previously mentioned boundary conditions to determine them:

- To ensure that the solution remains finite as z approaches 0, the constant C2 must be zero.
- On the wall z=0, we must have:

$$\theta(0,\mathrm{t}) = \text{ réelle } [C_1 \cdot \exp(\beta t)] = \text{ réelle } [C_1 \cdot (\cos(wt) + i \cdot \sin(wt))] = \mathrm{A} \cdot \cos[w\mathrm{t}] \qquad (19)$$

Noticing that:

$$\sqrt{i \cdot w} = \sqrt{\frac{w}{2}} \cdot (1 + i)$$

The complex solution of equation (18) can be written in the form:

$$\theta(\mathrm{z},\mathrm{t}) = \mathrm{A} \cdot \exp\left(-\sqrt{\frac{\omega}{2a}}(i+1) \cdot z\right) \cdot \exp(iwt) \qquad (20)$$

which transforms into:

$$\theta(\mathrm{z,t}) = \mathrm{A}\cdot\exp\left(-\sqrt{\frac{\omega}{2a}}z\right)\cdot\left[\exp(i\omega\cdot t)\cdot\exp\left(-i\sqrt{\frac{\omega}{2a}}z\right)\right] \quad (21)$$

Let's introduce the trigonometric form of the solution:

$$\theta(z,t) = A\cdot\exp\left(-\sqrt{\frac{\omega}{2a}}z\right)\cdot\left[(\cos\ \omega t + i\sin\ \omega t)\cdot\left(\cos\left(-\sqrt{\frac{\omega}{2a}}z\right) + i\sin\left(-\sqrt{\frac{\omega}{2a}}z\right)\right)\right] \quad (22)$$

After rearrangement, we will have:

$$\begin{aligned}\theta(z,t) &= A\cdot\exp\left(-\sqrt{\frac{\omega}{2a}}z\right)\cdot\left[\left(\cos(\omega t)\cdot\cos\left(-\sqrt{\frac{\omega}{2a}}z\right) + i\cos\ \omega(t-t_0)\cdot\sin\left(-\sqrt{\frac{\omega}{2a}}z\right) + \right.\right.\\ &\left.\left. i\sin(\omega t)\cos\left(-\sqrt{\frac{\omega}{2a}}z\right)\right) + i^2\sin(\omega t)\cdot\sin\left(-\sqrt{\frac{\omega}{2a}}z\right)\right]\\ \theta(z,t) &= A\cdot\exp\left(-\sqrt{\frac{\omega}{2a}}z\right)\cdot\left[\cos(\omega t)\cdot\cos\left(-\sqrt{\frac{\omega}{2\alpha}}z\right) - \sin(\omega t)\cdot\sin\left(-\sqrt{\frac{\omega}{2a}}z\right) + \right.\\ &\left. i\left(\cos(\omega t)\cdot\sin\left(-\sqrt{\frac{\omega}{2a}}z\right) + \sin(\omega t)\cdot\cos\left(-\sqrt{\frac{\omega}{2a}}z\right)\right)\right]\end{aligned} \quad (23)$$

The fluctuation of the desired temperature is the real part of the complex solution obtained, there for[34-42]:

$$\theta(z,t) = \mathrm{A}\cdot\exp\left(-\sqrt{\frac{\omega}{2a}}z\right)\cdot\left[\cos\omega(t-t_0)\cdot\cos\left(\sqrt{\frac{\omega}{2\alpha}}z\right) + \sin\omega t\cdot \sin\left(\sqrt{\frac{\omega}{2a}}z\right)\right] \quad (24)$$

Finally, the expression T(z,t) will take the following form:

$$T(z,t) = T_i + \mathrm{A}\cdot\exp\left(-\sqrt{\frac{\omega}{2a}}z\right)\cdot\cos\left(\omega t - \sqrt{\frac{\omega}{2\alpha}}z\right) \quad (25)$$

III. The thermal model of the water-earth heat exchanger:

III.1. System description:

A water-to-earth heat exchanger with five steel pipes, each measuring 30 meters, can be described as follows:

The heat exchanger consists of five parallel steel pipes, each having a length of 30 meters. The pipes are typically made of high-quality steel, known for its durability and excellent heat transfer properties.

Water circulates through these pipes as the working medium. The fluid enters the heat exchanger at a high temperature and flows through the individual pipes.

As the fluid flows through the pipes, it comes into contact with the surrounding earth, which acts as the heat sink, which is called cooling mode. The steel pipes facilitate the transfer of thermal energy between the fluid and the earth.

During the cooling mode, the water releases heat to the earth through the steel pipes. Heat is transferred from the fluid to the earth, again through conduction.

The length of 30 meters for each pipe provides an extended contact area between the fluid and the earth, enhancing the heat transfer efficiency. The parallel arrangement of the pipes allows for simultaneous heat exchange, further improving the overall performance of the system.

This water-to-earth heat exchanger with four steel pipes serves as a means to exchange thermal energy between the water and the earth, enabling effective heating or cooling in a geothermal system.

III.2. Steady-State Modeling of Water Temperature Along the Tube:

The energy balances between two tube sections separated by a distance of Δz can be expressed as follows:

$$\text{m. } c_{\text{pwater}} \cdot \frac{DT_a}{Dt} = q_1 - q_2 - q_3 \qquad (26)$$

Equation 26 represent the energy balances for water cooling, is:

$$q_3 = \frac{T_{\text{water}} - T_{\text{soil}}}{R_{\text{totale}}} \qquad (27)$$

based on the equation 27, we observe that the energy balance 26 for the operating cycle which is expressed as follows:

$$m \cdot c_{\text{pwater}} \cdot \left(\frac{\partial T_w}{\partial t} + u\frac{\partial T_w}{\partial x}\right) = -\lambda \cdot s \cdot \frac{\partial T_w}{\partial x}\Big|_X + \lambda \cdot s \cdot \frac{\partial T_w}{\partial x}\Big|_{X+\Delta X} + \frac{(T_{\text{soil}} - T_w)}{R_{\text{totale}}}$$

(28)

The average air flow velocity within the exchanger is denoted by 'u'. The overall thermal resistance of the system (R_{total}) is a combination of the thermal resistance due to soil (R_{soil}) and tube (R_{tube}) conduction, and the convective resistance offered by the water (R_{cv}).

$$R_{\text{totale}} = R_{\text{tube}} + R_{\text{tube}} + R_{cv} \qquad (29)$$

The thermal resistance of the tube is expressed as follows:

$$R_{\text{tube}} = \frac{1}{\lambda_{\text{tube}} \cdot 2\pi \cdot \Delta x} \ln\left(\frac{r2}{r_1}\right) \qquad (30)$$

The thermal resistance of the soil is given by equation (31):

$$R_{\text{soil}} = \frac{1}{\lambda_{soil} \cdot 2\pi \cdot \Delta x} \ln\left(\frac{r_3}{r_2}\right) \qquad (31)$$

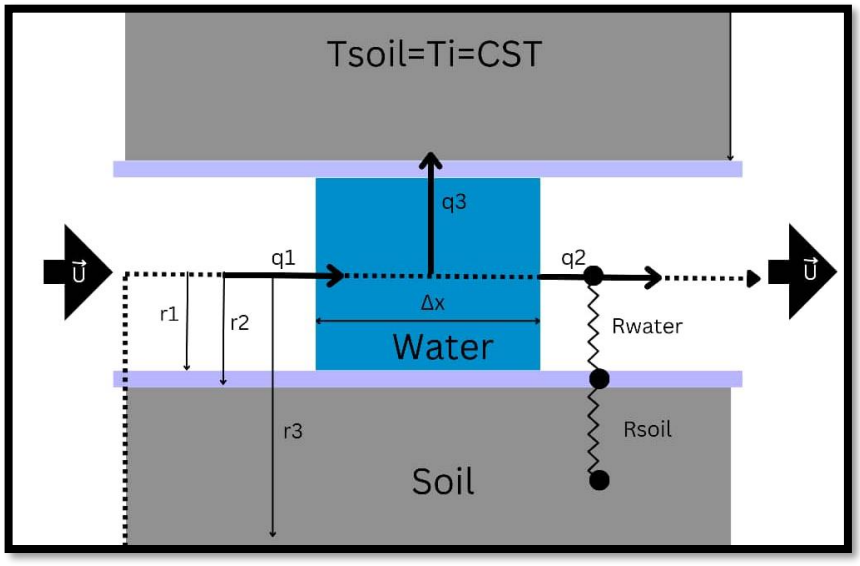

Figure 4 : Descriptive diagram of horizontal section II for a cooling cycle.

On the other hand, the thermal resistance of the water is expressed in the following form:

$$R_{\text{water}} = \frac{1}{h_{cv} \cdot 2 \cdot r \cdot \Delta x} \tag{32}$$

By dividing equation 28 by the differential element Δx, we obtain:

$$\rho . s \cdot c_{\text{pwater}} \cdot \left(\frac{\partial T_w}{\partial t} + u \frac{\partial T_w}{\partial x} \right) = \frac{-\lambda \cdot s \cdot \frac{\partial T_w}{\partial x}\Big|_x + \lambda \cdot s \cdot \frac{\partial T_w}{\partial x}\Big|_{x+\Delta x}}{\Delta x} + \frac{(T_{\text{soil}} - T_w)}{R_{\text{itotale}}} \tag{33}$$

To determine the convective heat transfer coefficient, one can use the Reynolds number (Re) and Nusselt number (Nu) which are provided as follows:

$$Re = \frac{\rho v_w 2r1}{\mu} \tag{34}$$

The Nusselt number for laminar flow is given as: Nu= 4.36 for Re < 2300 and Nusselt number for turbulent flow in a circular pipe for the ranges 0.5 < pr < 2000 and 2300 < Re < 5 * 10^6 is given as[43]:

$$Nu = \frac{(f/8)(Re - 1000)Pr}{1 + 12.7(f/8)^{0.5}(Pr^{0.66} - 1)} \tag{35}$$

here *f* is friction factor for smooth pipes and is calculated by Petu-khov's relation[44]:

$$f = (0.79 \ln \text{Re} - 1.64)^{-2}$$

Now the thermal resistance due to convective heat transfer between flowing water and inner surface of buried pipe is calculated as[44]:

where h is convective heat transfer coefficient and calculated as[44]:

$$h = \frac{Nu \lambda_w}{2r_{\text{I}}} \tag{36}$$

The total thermal resistance between flowing water and soil of EWHE system is calculated from:

$R_{\text{total}} = R_{\text{soil}} + R_{\text{pipe}} + R_{\text{Convec}}$

Then overall heat transfer coefficient is defined by:

$$U = \frac{1}{R_{\text{total}}} \tag{37}$$

For a pipe of constant temperature ($T_{pipesurface} = T_s$) the effectiveness of EWHE can be calculated as[45]:

$$\varepsilon = 1 - e\left(\frac{U}{\dot{m}_w c_{pw}}\right) \quad (38)$$

$\dot{m}_w$: mass flow rate of water (kg/s)

Then the temperature effectiveness is calculated as[45]:

$$\varepsilon = \frac{T_{win} - T_{wou}}{T_{win} - T_s} \quad (39)$$

Let, $R_{itotale}$ be the total thermal resistance per unit length.

$$\rho.S.c_{pwater} \cdot \left(\frac{\partial T_w}{\partial t} + u\frac{\partial T_w}{\partial z}\right) = \lambda \cdot s \cdot \frac{\partial^2 T_w}{\partial z^2} + \frac{(T_{soil} - T_w)}{R_{itotale}} \quad (40)$$

Assuming that Δz tends to 0 and taking into account that the transfer is steady-state and dominated by convection over conduction, equation (6) reduces to:

$$\rho \cdot \pi \cdot r_1^2 \cdot c_{pwater} \cdot u\frac{dT_w}{dz} = \frac{(T_{soil} - T_w)}{R_{itotale}} \quad (41)$$

Then:

$$\rho \cdot \pi \cdot {r_1}^2 \cdot c_{pwater} \cdot u\frac{dT_w}{dx} = \frac{(T_{soil} - T_w)}{R_{itotale}} \quad (42)$$

And:

$$\ln(T_w - T_{soil}) = -\left(\frac{1}{\rho \cdot \pi \cdot r_1^2 \cdot c_{pwater} \cdot R_{itotale}}\right)x + C \quad (43)$$

With:

$$T_w(x = 0) = T_{win}$$

Where T_{win} is the temperature at the inlet EWHE. There fore, the temperature profile is written in the following form:

$$T_w(x) = T_{soil} + (T_{win} - T_{soil}) \cdot \exp\left[-\frac{1}{\rho \cdot \pi \cdot r_1^2 \cdot c_{pwater} \cdot R_{itotale} \cdot U}x\right] \quad (44)$$

- **Effective efficiency of the brakes:**

As a result effective efficiency of the brakes can be calculated according to this formula[46]:

$$\epsilon = \frac{Q}{Q_{max}} \qquad (45)$$

Where: $Q = \dot{m} c_p (T_{in} - T_{ou})$

and $Q_{max} = \dot{m} c_p (T_{brakes} - T_{ou})$

By substitution:

$$\epsilon = \frac{(Tin - Tou)}{(Tbrakes - Tou)} \qquad (46)$$

Chapter IV

Theoretical Study, Results and Discussions

I. Introduction:

In this chapter, the outcomes of the mathematical models created in chapter three are discussed.

Initially, temperature profiles for three distinct soil types are depicted to determine the ideal depth for burying the pipe and the appropriate soil type for the water-ground heat exchanger system.

Subsequently, a verification process will be conducted to validate the numerical results with experimental outcomes found in literature and with other results presented in chapter four.

Lastly, the impact of various thermo-physical and geometric factors on the thermal performance of the water-ground heat exchanger will be explained (all the results were found using MATLAB 2023 Ra).

II. Thermal Model of the Soil:

2.1 Temperature profile of the soil:

Figures 1, 2, and 3 illustrate the average annual variation in soil temperature for three different types of soil. Table 1 represents the various thermophysical properties of the three types of soil studied (moist sand, clay, and clay-silt loam). It can be observed that the average soil temperature decreases as one penetrates further into the ground. This behaviour is evident in the soil with low thermal diffusivity (Fig. 1) compared to the other types of soil (Figs. 2 and 3). The type of soil plays a crucial role in the burial and operation of the air-to-soil heat exchanger.

Table 1. Thermophysical properties of different types of soil.

Nature du sol	**Conductivité thermique λ_{sol} (W/m.K)**	**Chaleur spécifique C_p (J/kg.K)**	**Masse volumique ρ (kg/m3)**
Sable humide	0,58	1000	1750
Argile	1,25	880	1450
Limon argilo-sableau	1,5	1340	1800

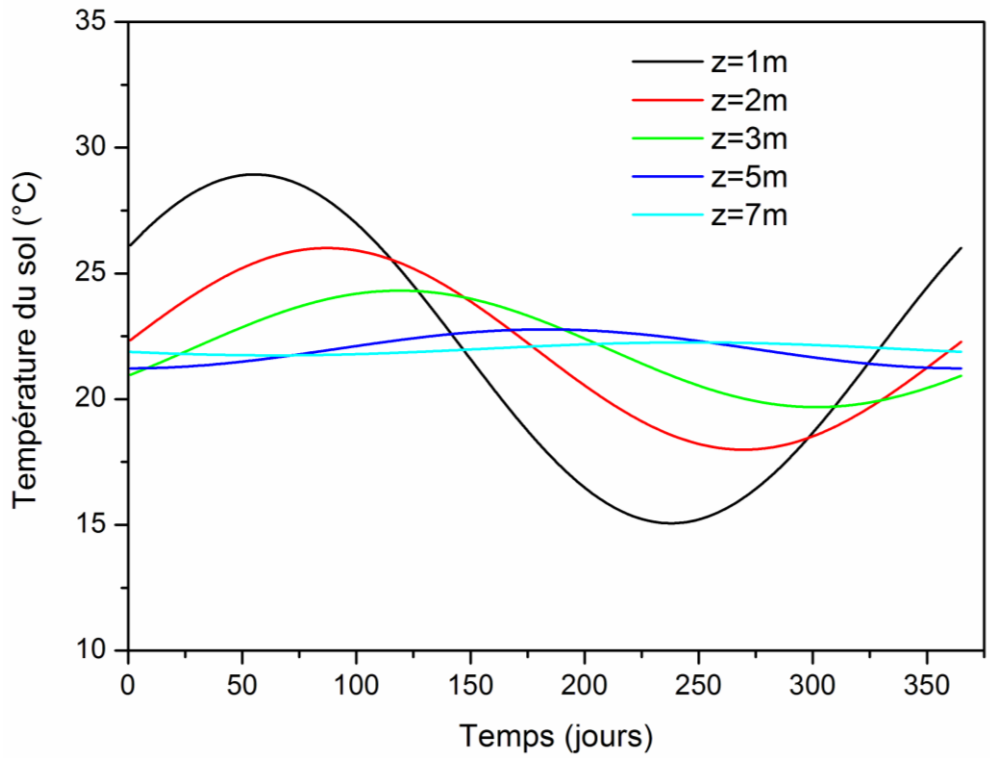

Figure I: Hourly evolution of soil temperature as a function of depth for a moist sand soil.

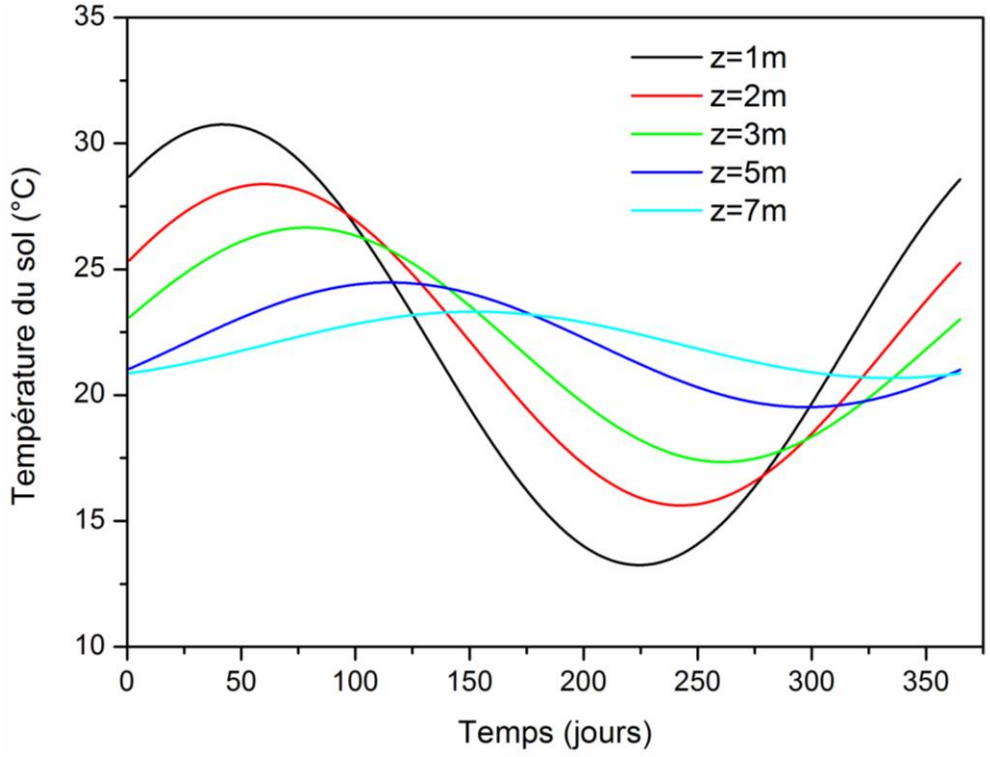

Figure II: Hourly evolution of soil temperature as a function of depth for a clay soil.

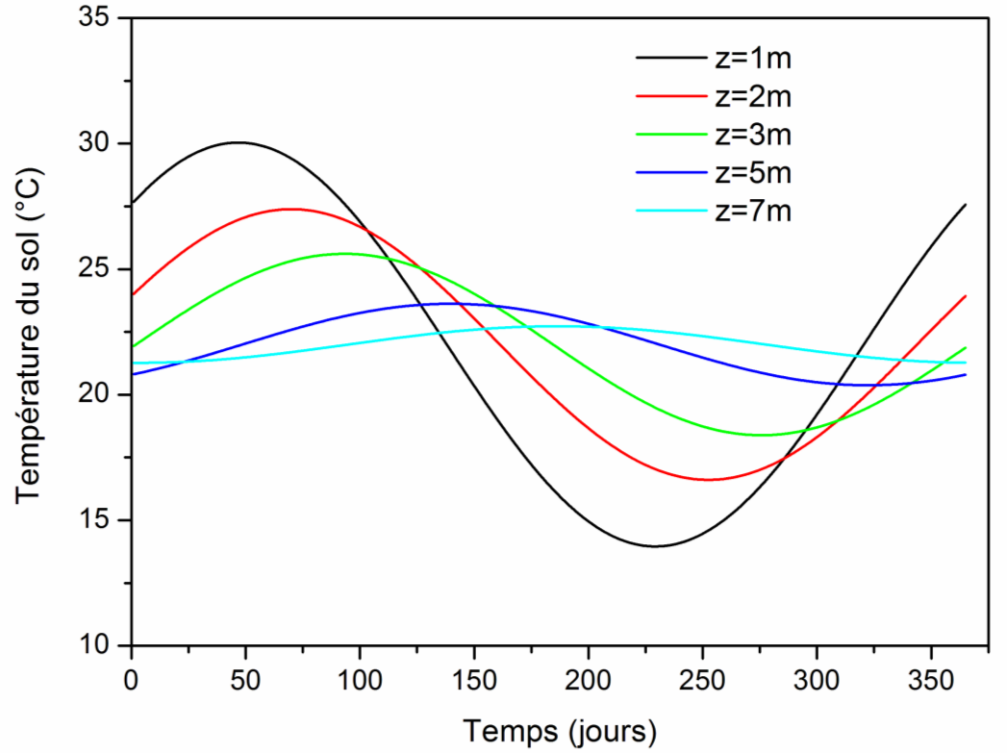

Figure III : Hourly evolution of soil temperature as a function of depth for a clay-silt loam soil.

III. Thermal Model of the Ground water Heat Exchanger:

III.1. Validation of the numerical model developed through experimentation:

The numerical model designed to investigate the air temperature variations along the ground-air geothermal heat exchanger has been validated by Belloufi et al [1] through experimentation. The validation process utilized two flow velocities (U_1, U_2 and U_3 :2, 3.5 and 4.5 m/s respectively), which are listed in the table below:

The graph (Figure 1) indicates that the theoretical and experimental results match well when a flow velocity of 2 m/s is used.

by varying the inlet temperatures to the heat exchanger 45.53 C°, 36.53 C° and 42.78 C°, the relative errors were found to be around 5.01%, 5.1%, and 4.7% respectively.

This can be concluded that the model developed is accurate and can be used for more detailed analysis.

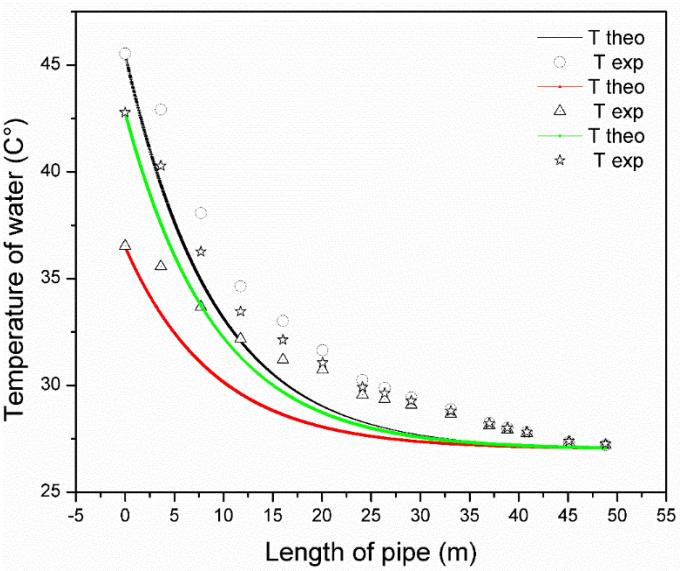

Figure 1 : Validation of theoretical result with experimental result of Belloufi et al [47] (U = 2m/s)

By analyzing the graphs (Figure 2 and 3) , it can be observed that the theoretical and experimental data align well when the flow velocity is set to 3.5 m/s and 4.5 m/s. When the inlet temperatures to the heat exchanger are varied to 34.83 C°, 42.56 C°, and 47.29 C° for 3.5 m/s and 32.73°C, 41.7°C, and 35.85°C for 4.5 m/s flow velocity, the relative errors are calculated to be approximately 4.22%, 5.62%, 5.56%, and 9.78%, 8.45%, 9.86% respectively. Therefore, it can be concluded that the developed model is precise and can be applied for more comprehensive analyses.

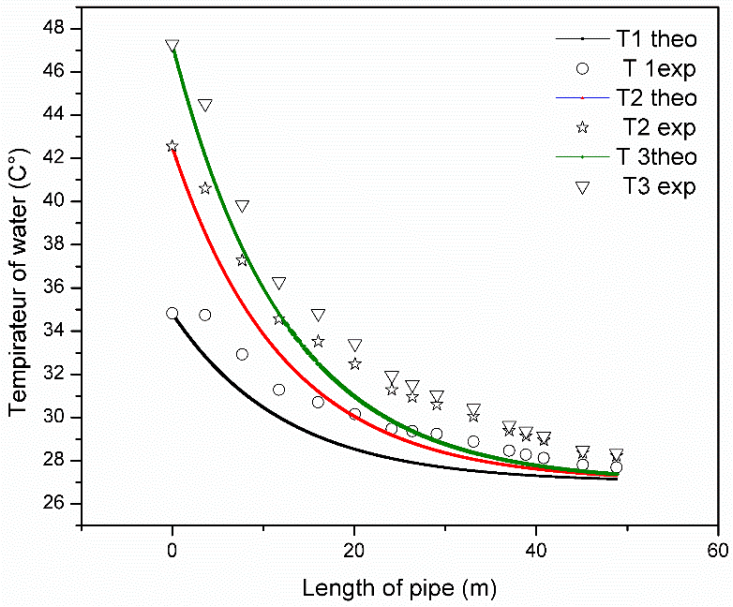

Figure 2 : Validation of theoretical result with experimental result of Belloufi et al [47] (U = 3.5m/s)

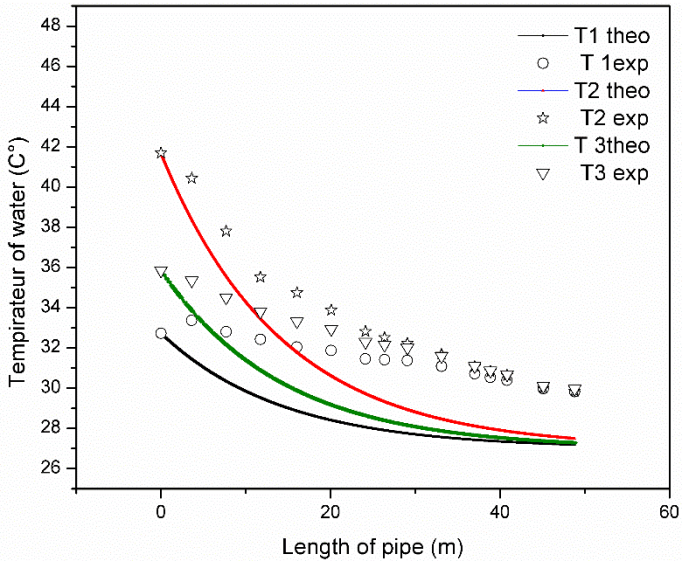

Figure 3 : Validation of theoretical result with experimental result of Belloufi et al [47] (U = 4.5m/s)

Table 2. Key parameters of the water-to-ground heat exchanger used for validation:[47]

Physical and thermal parameters	**Values**
air density (kg/m3)	1.2
air flow velocity (m/s)	3.5
Internal diameter of the pipe (m)	0.1
Pipe thermal conductivity (W/m. ◦C)	0.17
Soil thermal conductivity (W/m. ◦C)	1. 25
Specific heat capacity of air (J/Kg. ◦C)	1000
Undisturbed soil temperature (◦C)	26

IV. Parametric study:

The purpose of this parametric investigation is to assess how the thermophysical and geometrical parameters of the water-ground heat exchanger affect its thermal efficiency. The various features utilized in this analysis are depicted in the table.

To elucidate the impact of the different parameters on the thermal performance, a steady temperature is enforced at the tube's inlet.

Table 3. Characteristics used in the parametric study of the ground-water heat exchanger.

System	Value
Temperature of the soil	27 °C
Inlet water temperature	60 °C
Water flow velocity	0.466 m/s
Thermal conductivity of the soil	1,5 W/(m.°C)
Burial depth of EWHE	3 m
Length of the pipe	30 m
Inner radius of the tube r1	5 mm
Tube thickness	1 mm
Thermal conductivity of the tube λp	47.5 W/(m.°C)
Specific heat capacity of the water	4186(Kg.°C)

IV.1. Effect of water flow velocity:

Four water flow velocities (0.466m/s,0.9 m/s, 1.2 m/s) are considered for the analysis of the effect of continuous operating mode on thermal performance.

The following graph (Figure 4) shows the variations of the temperature of the flowing water inside the water-ground heat exchanger tube as a function of the length of the tube, where each curve corresponds to a different flow velocity. It can be observed that at a flow rate of 1.2 m/s, the water temperature decreases regularly (by approximately 0.5°C per half meter) from 60°C to 35.64°C at the end of the heat exchanger tube, which is after 30 meters. However, at flow rates of 0.466 and 0.9, the temperature drops to 27.96°C and 32.63°C, respectively.

As shown by the graph of the column chart (Figure 5), the effectiveness of the heat exchanger increases as the water flow rate decreases. therefore increasing the water flow velocity leads to a significant reduction in the time required to cool it. These results suggest that higher flow velocities result in less of a temperature drop.

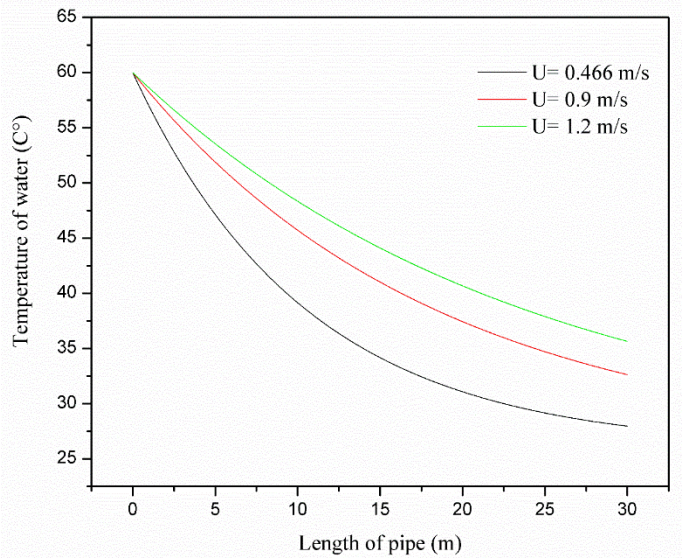

Figure 4 : .Effect of water flow velocity on its temperature drop along the water-ground heat exchanger

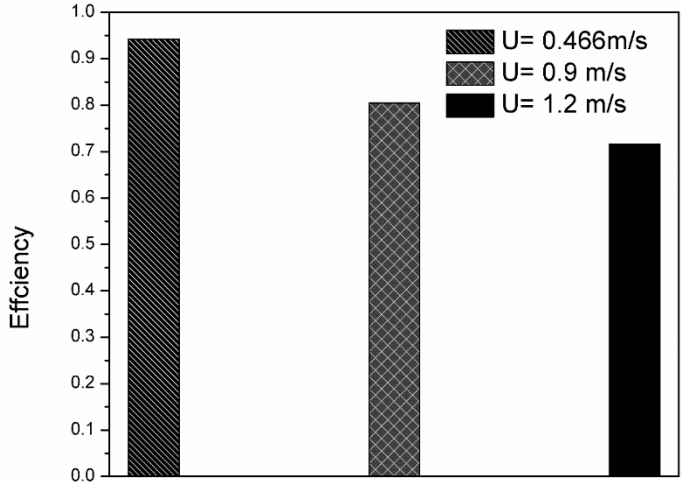

Figure 5: Effect of water flow velocity on the efficacy of EWHE

IV.2. Effect of the thermal conductivity of the tube:

The following graph (Figure 6) illustrates the effect of the thermal conductivity of the material used to manufacture the water-ground heat exchanger tube on the temperature changes of the flowing water inside along its length. At the end of the pipe, water flows at different temperatures of 27.92°C, 27.96°C, and 41.23°C, depending on the thermal conductivity of each tube, which is 237, 47.5, and 0.165 (w/m. k), respectively.

For aluminium and iron materials, we notice the similarity of the two graphs, indicating no significant difference in the temperature drop, unlike the PVC material which maintained the water at a high temperature along the tube.

As shown by the graph of the column chart (Figure 7), the effectiveness of the heat exchanger increases with high thermal conductivity, such as metals, which allows higher heat exchange between water and the ground compared to other materials, allowing for cooling to achieve the desired temperature ranges.

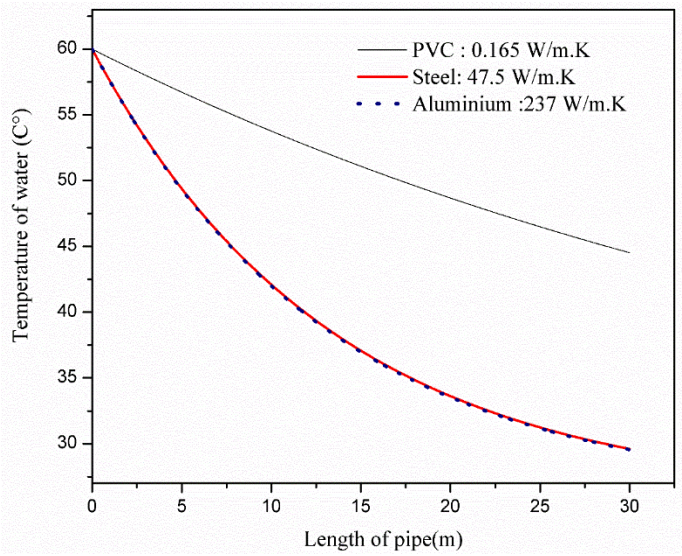

Figure 6: Effect of Thermal Conductivity Variation on Temperature Change of Water Along Water-Ground Heat Exchanger Tube

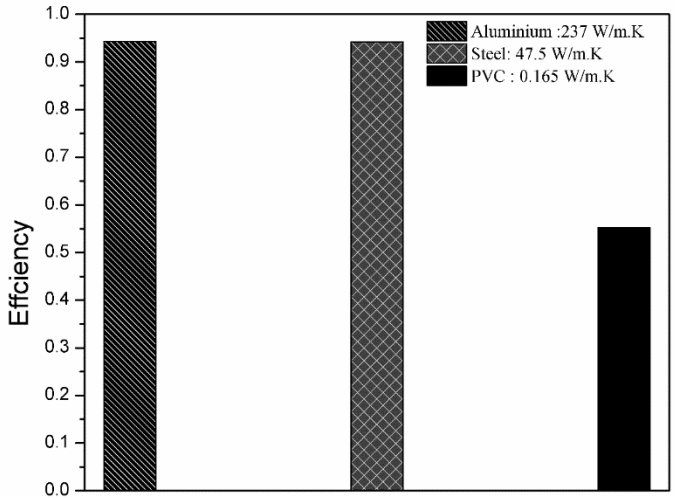

Figure 7: Effect of Thermal Conductivity Variation on the efficiency of EWHE

IV.3. Effect of the tube diameter:

Three different pipe radiuses (0.005 m, 0.007 m, and 0.01 m) were considered to examine the thermal performance. A water velocity of 0.466 m/s and a thermal conductivity of 47.5 (w/m.k) of steel were kept constant for all four tube diameters.

The following graph (Figure 8) illustrates the effect of changing the radius of the tube in a water-ground heat exchanger on the flowing water temperature. It is observed that the rate of temperature decrease is significantly related to the tube radius. When the radius is 0.01 meters, there is a small decrease in temperature (from 60 to around 43.02 degrees Celsius). Therefore, the smaller the tube radius, the more effective the water cooling, As shown by the graph of the column chart (Figure 9), For example, when the radius is 0.005 meters, the temperature drops to around 27 degrees Celsius.

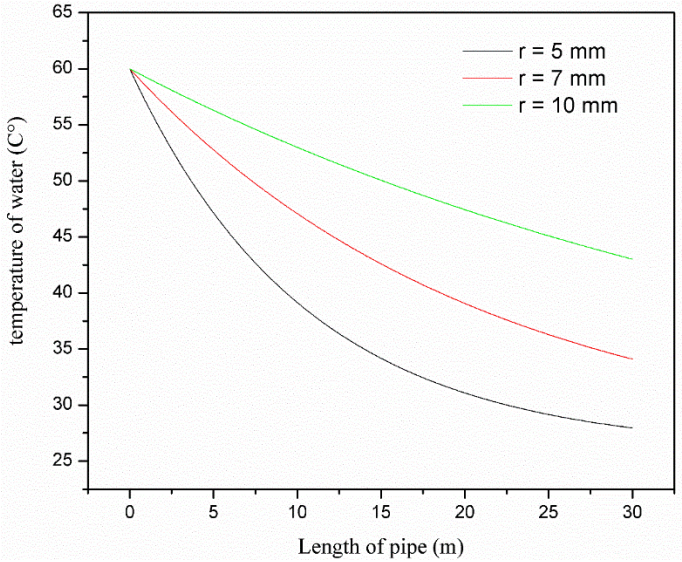

Figure 8: The effect of changing the radius of the water-ground heat exchanger tube on the change in the temperature of the flowing water along the tube.

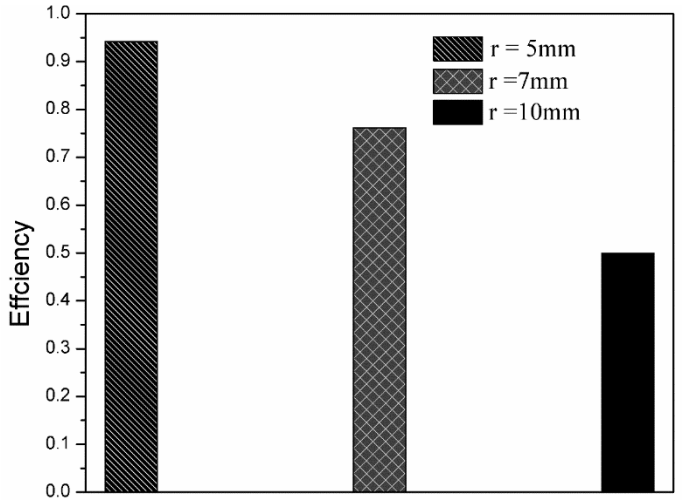

Figure 9: The effect of changing the radius of the water-ground heat exchanger tube on its efficiency

IV.4. Effect of soil thermal conductivity:

Three different thermal conductivities (0.7W/m.K, 1.25W/m.K, and 1.5 W/m.K) are considered to evaluate the thermal performance and determine the optimal soil conductivity for burying the heat exchanger.

Through the graphical curves (Figure 10), it can be observed that the rate of temperature drop of the water along the tube varies with the thermal conductivity of the soil. When the thermal conductivity is fixed at 0.7 W/m.K, the water temperature on the tube decreases at a relatively low rate (from 60 to 33.59 °C). when thermal conductivity increases, Earth becomes more capable of transferring heat. This leads to an increase in the amount of heat that can be transferred from the Earth to the water within a specific time period. When heat exchange occurs more effectively and quickly, the water is cooled more efficiently. for example, when fixing it at 1.25 and 1.5, where the water was cooled to lower temperatures of 28.89°C and 27.96 °C, respectively.

Therefore, the cooling of water at the water-ground heat exchanger will be better as the thermal conductivity of the buried soil increases, The column chart graph provides an explanation for the observed trend. (Figure 11).

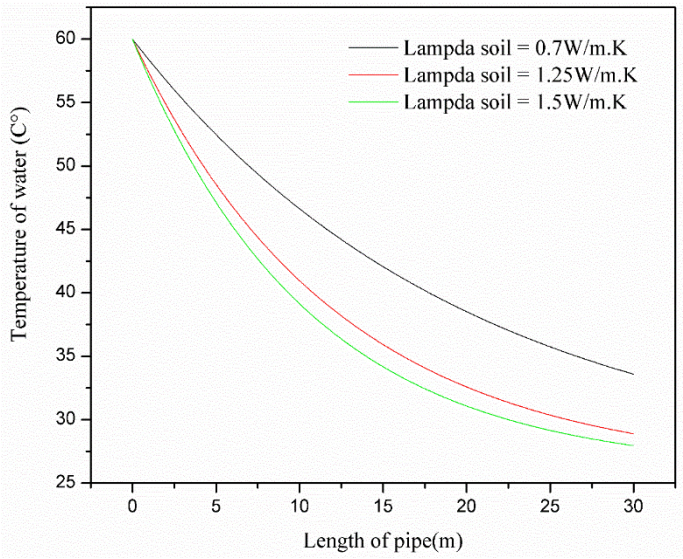

Figure 10: The effect of changing the thermal conductivity of the soil on the temperature changes of water along the water-ground heat exchanger tube.

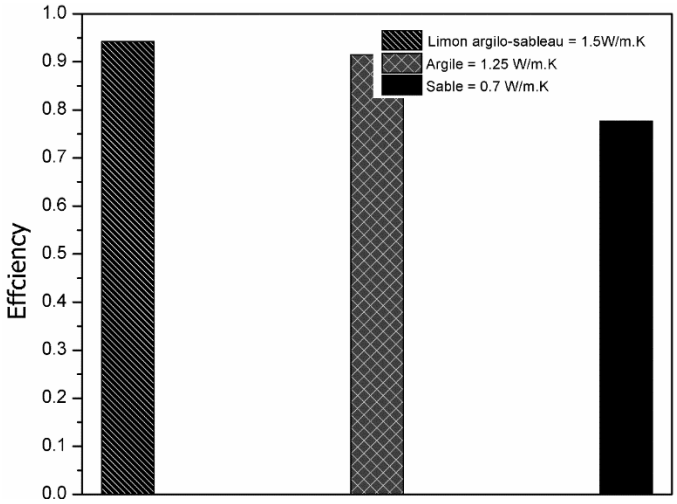

Figure 11: The effect of changing the thermal conductivity of the soil on the. the efficiency of EWHE

IV.5. Effect of the temperature at inlet of EWHE:

The effect of changing the water temperature at the inlet of the water-ground heat exchanger tube on the outgoing water temperature was measured three times (at 50, 60, and 70 degrees Celsius) to assess its impact.

It is evident that when water is introduced at 50 degrees Celsius, there is a noticeable decrease in temperature along the tube until it reaches 27.38 degrees Celsius. However, at inlet temperatures of 60 and 70 degrees Celsius, the rate of cooling is higher, resulting in temperatures close to those obtained previously at the tube outlet, where temperatures of 27.96 and 28.54 degrees Celsius were recorded, respectively. Therefore, it can be concluded that the higher the temperature at the tube inlet, the more effective the water-ground heat exchanger is in cooling the water.

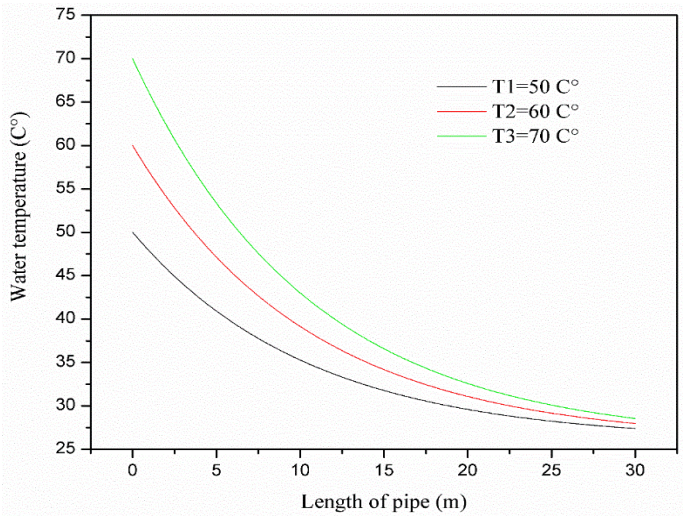

Figure 12: The effect of changing the inlet water temperature on the variations of temperature along the water-ground heat exchanger pipe

V. The effectiveness of the brakes:

The main idea conveyed by the given curves is that the efficiency of the brakes shows a noticeable improvement when utilizing the water-soil heat exchanger compared to the standard braking system without the exchanger. Moreover, the effectiveness of the brakes is directly related to the efficiency of the heat exchanger. In other words, as the heat exchanger becomes more efficient, the brakes exhibit higher levels of effectiveness. These conclusions were drawn based on a comprehensive analysis of various criteria that were previously investigated. Overall, the curves demonstrate the positive impact of incorporating the water-soil heat exchanger on the performance and efficiency of the braking system.

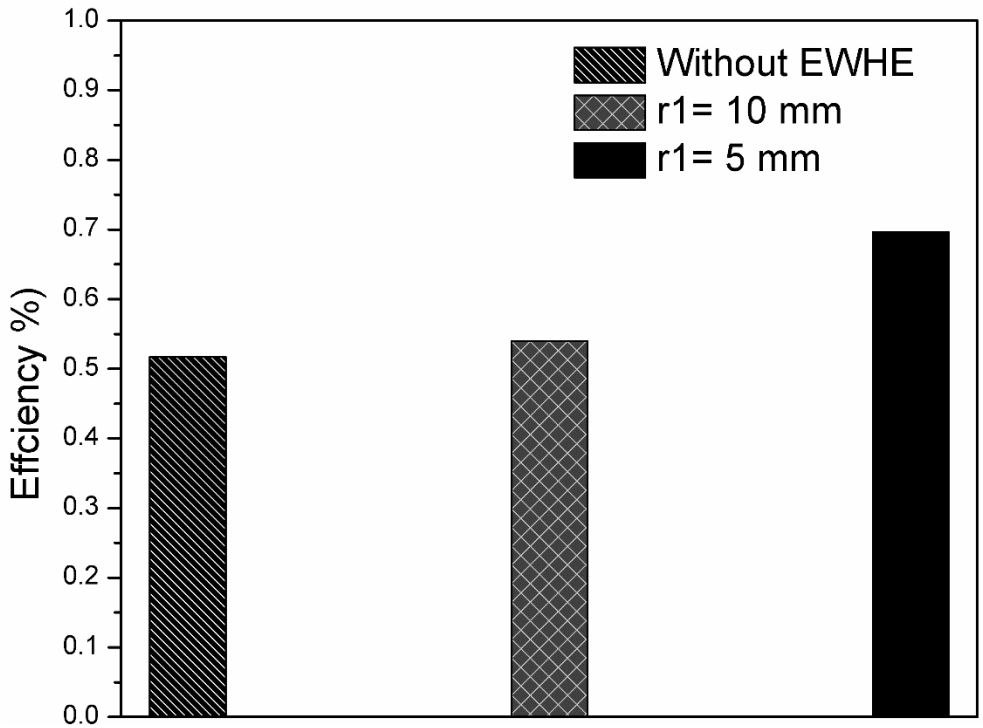

Figure 13: A bar chart illustrates the relationship between brake efficiency and the radius of the water-soil heat exchanger tube

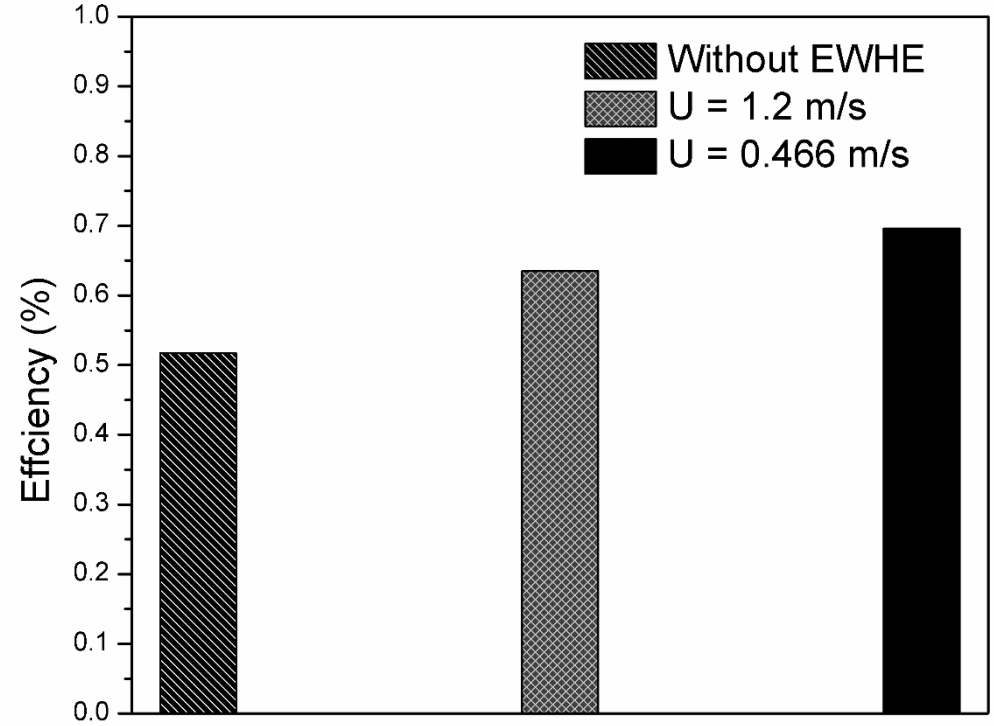

Figure 14: A bar chart illustrates the relationship between brake efficiency and the velocity of the water in the heat exchanger tube

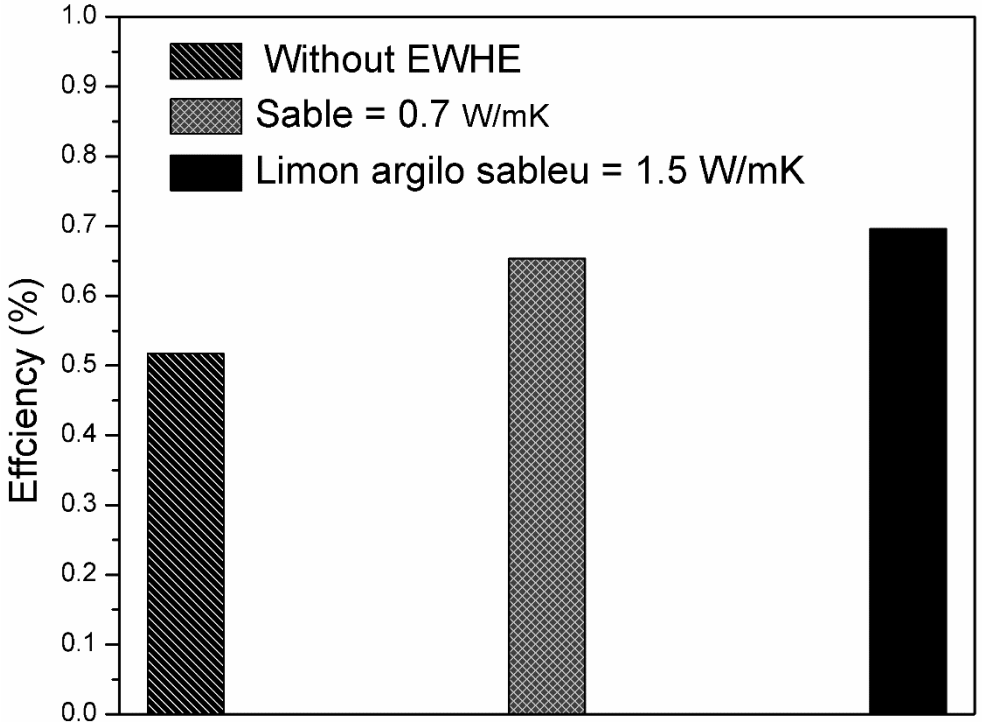

Figure 15: A bar chart illustrates the relationship between brake efficiency and the thermal conductivity of the soil

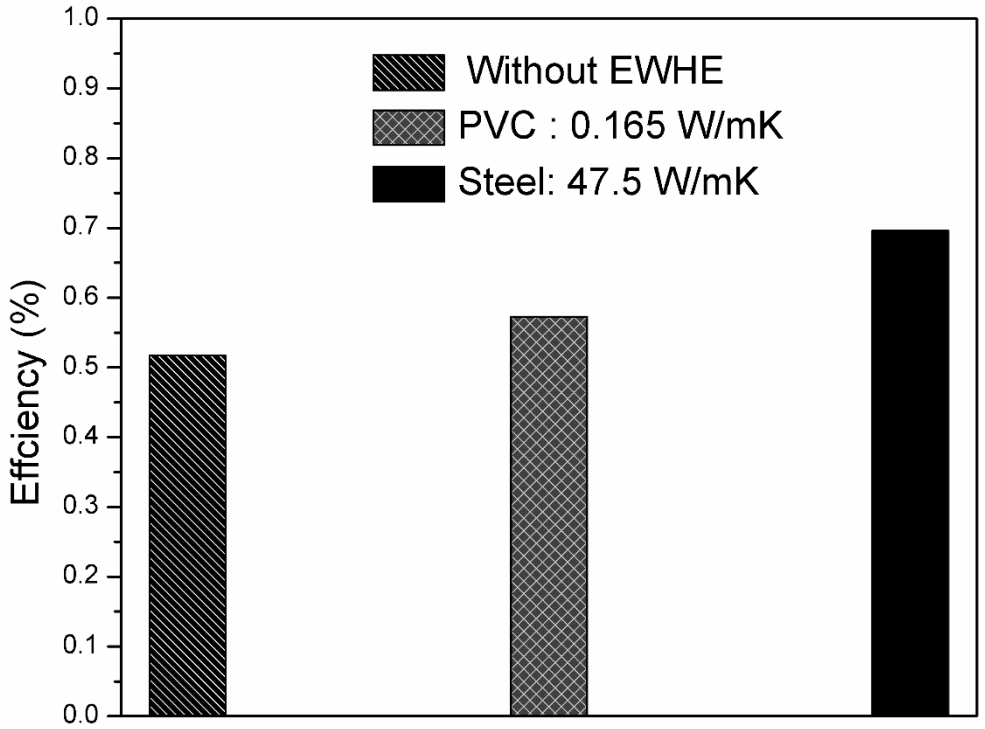

Figure 16: A bar chart illustrates the relationship between brake efficiency and the thermal conductivity of the pipe

In conclusion,

The analysis of existing literature in Chapter 2 highlighted the benefits and challenges associated with the integration of EWHE technology in drawworks braking systems. The literature review revealed that the adoption of EWHE systems offers enhanced control and response, allowing for precise and rapid braking actions. Moreover, the use of EWHE reduces the reliance on traditional systems, resulting in decreased energy consumption and lower environmental impact.

Chapter 3 focused on the mathematical modeling and numerical simulation of the EWHE braking system in drawworks. By developing accurate mathematical equations and utilizing numerical methods, researchers were able to analyze and optimize the performance of the braking system. The simulation results demonstrated improved braking efficiency and stability, contributing to enhanced operational safety and productivity.

The experimental investigations conducted in Chapter 4 provided real-world validation of the theoretical aspects discussed in previous chapters. The experiments confirmed the feasibility and effectiveness of the EWHE braking system in drawworks, showcasing its superior performance compared to conventional hydraulic systems. The experimental results showcased the system's reliability, responsiveness, and capability to handle varying loads and operating conditions.

The findings from this research highlight the potential of EWHE technology in revolutionizing the braking systems of drawworks. The integration of EWHE systems offers numerous benefits, including increased efficiency, reduced energy consumption, enhanced control, and improved safety. These advancements have the potential to significantly enhance drilling operations in the oil and gas industry, leading to cost savings, increased productivity, and minimized environmental impact.

It is important to note that while this research has provided promising results, further studies and practical implementations are necessary to fully explore the potential of EWHE technology in drawworks braking systems. Continued research efforts should focus on optimizing system design,

improving control algorithms and conducting long-term field trials to validate the performance and durability of EWHE systems.

In conclusion, the amelioration of the braking system in drawworks using EWHE technology presents a promising avenue for enhancing drilling operations. The integration of EWHE systems

can revolutionize the efficiency, safety, and sustainability of drawworks, leading to improved overall performance and reduced environmental impact. The findings from this research contribute to the growing body of knowledge in this field and provide a foundation for further advancements and practical implementations of EWHE technology in the oil and gas industry.

In summary, the key findings of the research presented in this thesis can be summarized in the following five important points:

- The effectiveness of the water-earth heat exchanger decreases as the water flow rate inside the exchanger increases.
- The efficiency of the heat exchanger increases with a larger diameter of the exchanger tube.
- The cooling performance of the water is improved with an increase in the thermal conductivity of the metal used in the manufacturing of the water-earth heat exchanger tube.
- The effectiveness of the heat exchanger increases with a higher thermal conductivity of the earth.
- There is a direct relationship between the efficiency of the braking system and the efficiency of the water-earth heat exchanger. As the efficiency of the heat exchanger increases, the efficiency of the braking system also increases, and vice versa.

The end.

❖ Sources and references :

1. Dyke, K.V., *The Drawworks and the Compound Unit 1, Lesson 6*. rotary drilling series. August 1, 1995, Texas at Austin: The University of Texas at Austin - Petroleum Extension Service.
2. Division, N.S., *NATIONAL*

DRAWWORKS

TYPE1625-DE, in *Parts list*. JAN. l, 1969 Houston-, T exes
3. University, E.C., *LIBYA – DRILLING & COMPLETION ENGINEER*. DRILLING RIGS 10/11/2006.
4. institutpetroleum, P.E.a.d.r., *OPERATION, MAINTENANCE AND PART MANUALS* in *JC-70 DB Drawworks*, B.O.M.D. LTD, Editor.: reqiu city , hebei province ? china.
5. ARBAOUI+BARCHE+KHERFI.
6. Walton, G.W., *DRAWWORKS TRANSMISSION*, U.S.P. OFFICE, Editor. 1943: UNITED STATES OF AMERICA. p. 3.
7. L'Espoir, J., *Drawworks Clutches*. transfer of technologies - expended series October 2009 Water Well Journal. 9.
8. SERIDI, N., *Utilisation d'outils au service de la maintenance*

d'un Treuil de forage OIL WELL 840E, in *Faculté des Sciences de l'Ingéniorat*

Département de Génie Mécanique. 2016-2017, UNIVERSITE BADJI MOKHTAR ANNABA. p. 54.
9. Atwany, H., et al., *Performance of earth-water heat exchanger for cooling applications.* 2019. **5**(1): p. 17-21.
10. Traoré, E.S., Y. Coulibaly, and T. Woodson. *Earth-Air Heat Exchangers for Passive Air Conditioning: Case Study Burkina Faso*. 2009.
11. Darius, D., et al. *Working parameters affecting earth-air heat exchanger (EAHE) system performance for passive cooling: A review*. in *IOP Conference Series: Materials Science and Engineering*. 2017. IOP Publishing.
12. Dakhil, A.A. and S.H.J.B.J.f.E.S. Hammadi, *Theoretical and Experimental Study of Water Storage Tank with Earth Water Heat Exchanger in Hot Climates Regions.* 2022. **22**(1).
13. Atwany, H., et al., *Experimental evaluation of ground heat exchanger in UAE.* Renewable Energy, 2020. **159**: p. 538-546.
14. Elminshawy, N.A., et al., *Experimental investigation of a V-trough PV concentrator integrated with a buried water heat exchanger cooling system.* 2019. **193**: p. 706-714.
15. Hammadi, S.H.J.T.S. and E. Progress, *Tempering of water storage tank temperature in hot climates regions using earth water heat exchanger.* 2018. **6**: p. 157-163.
16. Hamdan, M.O. *Tapping to geothermal energy through a high performance earth-to-water heat exchanger design*. in *2018 5th International Conference on Renewable Energy: Generation and Applications (ICREGA)*. 2018. IEEE.
17. Kappler, G., et al., *Study of an earth-to-water heat exchange system which relies on underground water tanks.* 2019. **133**: p. 1236-1246.
18. Atwany, H., et al., *Evaluating thermal conductivity of desert sand under different initial physical properties.* 2018. **4**(6): p. 236-240.
19. Sivasakthivel, T., et al., *Experimental thermal performance analysis of ground heat exchangers for space heating and cooling applications.* 2017. **113**: p. 1168-1181.
20. Kim, M.-J., et al., *Thermal performance evaluation and parametric study of a horizontal ground heat exchanger.* 2016. **60**: p. 134-143.

21. Jakhar, S., M. Soni, and N.J.E.P. Gakkhar, *Performance analysis of earth water heat exchanger for concentrating photovoltaic cooling.* 2016. **90**: p. 145-153.
22. Li, M., et al., *The performance analysis of the Trough Concentrating Solar Photovoltaic/Thermal system.* Energy Conversion and Management, 2011. **52**(6): p. 2378-2383.
23. Xu, X., et al., *Thermal modeling of hybrid concentrating PV/T collectors with tree-shaped channel networks cooling system*. 2012. 1131-1138.
24. Sivasakthivel, T., et al., *Experimental study of thermal performance of a ground source heat pump system installed in a Himalayan city of India for composite climatic conditions.* 2016. **131**: p. 193-206.
25. Rouag, A., et al., *Applicability of a solar adsorption cooling machine in semiarid regions: Proposal of supplementary cooler using earth-water heat exchanger.* 2016. **34**(2): p. 281-286.
26. Serageldin, A.A., et al., *The Effect of Groundwater Flow on the Thermal Performance of a Novel Borehole Heat Exchanger for Ground Source Heat Pump Systems: Small Scale Experiments and Numerical Simulation.* 2020. **13**(6): p. 1418.
27. Yang, L.-H., et al., *Enhanced efficiency of photovoltaic panels by integrating a spray cooling system with shallow geothermal energy heat exchanger.* Renewable Energy, 2019. **134**: p. 970-981.
28. Choudhary, K., et al., *Comparative Life Cycle Assessments of Photovoltaic Thermal Systems with Earth Water Heat Exchanger Cooling.* Procedia CIRP, 2022. **105**: p. 255-260.
29. Jakhar, S., M.S. Soni, and N. Gakkhar, *Modelling and Simulation of Concentrating Photovoltaic System with Earth Water Heat Exchanger Cooling.* Energy Procedia, 2017. **109**: p. 78-85.
30. Li, C., et al., *Effect of inner pipe type on the heat transfer performance of deep-buried coaxial double-pipe heat exchangers.* Renewable Energy, 2020. **145**: p. 1049-1060.
31. Jakhar, S., M. Soni, and N. Gakkhar, *Exergy analysis of a photovoltaic thermal system with earth water heat exchanger cooling system based on experimental data.* International Journal of Exergy, 2017. **23**: p. 367-387.
32. Jakhar, S., M.S. Soni, and N. Gakkhar, *An integrated photovoltaic thermal solar (IPVTS) system with earth water heat exchanger cooling: Energy and exergy analysis.* Solar Energy, 2017. **157**: p. 81-93.
33. Yusubov, F. and A.J.J.T. Aliyev, *Temperature distribution in a drilling brake contact.* 2021. **31**: p. 28-45.
34. Pfafferott, J., *Evaluation of earth-to-air heat exchangers with a standardised method to calculate energy efficiency.* Energy and Buildings, 2003. **35**(10): p. 971-983.
35. Krarti, M., J.F.J.E.C. Kreider, and Management, *ANALYTICAL MODEL FOR HEAT TRANSFER IN AN UNDERGROUND AIR TUNNEL.* 1996. **37**: p. 1561-1574.
36. Stevens, J.W., *Optimal placement depth for air–ground heat transfer systems.* Applied Thermal Engineering, 2004. **24**(2): p. 149-157.
37. Abadie, M., et al., *Heating and Cooling Potential of Buried Pipes in South Brazil*. 2006.
38. Sharan, G. and J. Ratan, *Performance of Single Pass Earth-Tube Heat Exchanger: An Experimental Study.* Indian Institute of Management Ahmedabad, Research and Publication Department, IIMA Working Papers, 2003. **40**.
39. Jacovides, C.P. and G. Mihalakakou, *An underground pipe system as an energy source for cooling/heating purposes.* Renewable Energy, 1995. **6**(8): p. 893-900.
40. Shukla, A., G. Tiwari, and M. Sodha, *Parametric and experimental study on thermal performance of an earth–air heat exchanger.* International Journal of Energy Research, 2006. **30**: p. 365-379.
41. Costa, V.A.F., *Thermodynamic analysis of building heating or cooling using the soil as heat reservoir.* International Journal of Heat and Mass Transfer, 2006. **49**(21): p. 4152-4160.
42. Cucumo, M., et al., *A one-dimensional transient analytical model for earth-to-air heat exchangers, taking into account condensation phenomena and thermal perturbation from the upper free*

surface as well as around the buried pipes. International Journal of Heat and Mass Transfer, 2008. **51**(3): p. 506-516.
43. Holman, J.P., *Heat transfer*. 2010: McGraw Hill Higher Education.
44. Incropera, F.P., et al., *Fundamentals of heat and mass transfer*. Vol. 6. 1996: Wiley New York.
45. Al-ajmi, F.F., et al., *The cooling potential of earth-air heat exchangers for domestic buildings in a desert climate.* 2006. **41**: p. 235-244.
46. Dobre, A., et al., *Recuperative braking drawworks.* EEA - Electrotehnica, Electronica, Automatica, 2018. **66**: p. 135-142.
47. Belloufi, Y., et al., *Transient assessment of an earth air heat exchanger in warm climatic conditions.* 2022. **104**: p. 102442.

Abstract:

This message presents a study that explores the utilization of a heat exchanger (water/soil) to cool the brake system in a driveworks system. The primary aim is to ensure a consistent distribution of heat within the soil along the water channel by applying the heat conduction equation and energy balance. An analytical model was proposed to determine water temperatures across the exchanger under a constant heat transfer condition, while a numerical model utilizing the finite difference method was developed for convective heat transfer. To validate the accuracy of both analytical and numerical models, an experimental study was conducted at the University of Ouargla, yielding qualitative and quantitative agreement during the verification process. Positive outcomes were observed in terms of improving the brake system's efficiency.

Keywords: Water-Soil Heat Exchanger, Brake Cooling, Analytical Equations, Increased System Efficiency.

ملخص :

تتناول هذه الرسالة دراسة استخدام المحول الحراري من نوع (ماء/تربة) في عملية تبريد فرامل نظام الدراووركس. الهدف الرئيسي هو تحقيق توزيع متساوٍ للحرارة داخل التربة على امتداد القناة المائية باستخدام معادلة الحرارة والحوصلة الطاقوية. تم اقتراح نموذج تحليلي لتحديد درجات حرارة المياه عبر المحول في حالة نقل الحرارة الثابتة، وتم تطوير نموذج عددي للنقل الحراري الانتقالي باستخدام طريقة الفروق المنتهية الضمنية. تم إجراء دراسة تجريبية في جامعة ورقلة للتحقق من صحة النماذج التحليلية والعددية المستخدمة، وتم تحقيق توافق نوعي وكمي خلال عملية التحقق. تم تحقيق نتائج إيجابية في زيادة كفاءة نظام المكابح .

الكلمات المفتاحية: المحول الحراري ماء-ارض، تبريد الفرامل، الدراووركس، المعادلات التحليلية، زيادة كفاءة النظام.